Check for updates

ChemCatChem

Research Article
doi.org/10.1002/cctc.202400013

Chemistry Europe
European Chemical Societies Publishing

www.chemcatchem.org

Selective Partial Reduction of Nitroarenes to the Hydrazoarene Catalyzed by Amine-Modified Ordered Mesoporous Silica Immobilized Ionic Liquid (OMSIIL) Stabilised RuNPs

S. Doherty,*[a] J. G. Knight,*[a] A. A. Alharbi,[a] C. Wills,[a] C. Dixon,[a] C. Cheng,[b] F. Russo Abegão,[c] T. W. Chamberlain,*[d] H. Yan,[d] A. Griffiths,[d] R. A. Bourne,[d] S. M. Collins,[d] K.-J. Wu,[d] and H. Alshaikh.[e]

This article is dedicated to the memory of Professor Stephen A. Westcott, a great ambassador for chemistry in Canada and across the globe and the best and most sincere of friends.

Ruthenium nanoparticles stabilised by an amine-modified Ordered Mesoporous Silica Immobilized Ionic Liquid (OMSIIL) are efficient catalysts for the partial reduction of nitrobenzene to hydrazobenzene with 100% selectivity as well as the complete reduction to aniline. High selectivity for the partial reduction of nitrobenzene to hydrazobenzene was obtained when the reaction was conducted in ethanol with 0.5 mol% catalyst and $NaBH_4$ as the hydrogen donor whereas aniline was obtained as the sole product in water when dimethylamine borane (DMAB) was used as the hydrogen donor. Interestingly, while a range of electron poor nitroarenes were reduced to the corresponding hydrazoarene with high selectivities and good conversions, nitroarenes substituted with electron donating groups resulted in complete reduction to the aniline. Composition-time profiles suggest that reductions conducted in ethanol with sodium borohydride occur via the condensation pathway while those conducted in water using dimethylamine borane as the hydrogen source may well go via the direct pathway. This is the first example of the selective reduction of nitrobenzene to hydrazobenzene using a ruthenium nanoparticle-based catalyst and the initial TOF of 320 mol nitrobenzene converted mol Ru^{-1} h^{-1} for the partial reduction of nitrobenzene to hydrazobenzene is markedly higher than previous literature reports. A study of the catalyst performance as a function of the surface modification revealed that each component has a direct and dramatic effect on the efficacy as RuNPs stabilised by COK-12 modified with imidazolium-based ionic liquid and a primary amine gave the highest conversion while selective removal of either component or replacement of the primary amine with a tertiary amine resulted in a marked reduction in efficiency.

Introduction

The reduction of nitroarenes to the corresponding aryl amine is a fundamentally important reaction as anilines are key motifs in a range of bioactive compounds and herbicides as well as intermediate in the production of fine chemicals and pigments as well as monomers for the synthesis of speciality polymers.[1] While the Buchwald-Hartwig based *N*-arylation has proven to be an extremely powerful and highly versatile tool for the synthesis of an architecturally diverse range of aryl and heteroaryl amines,[2] the transfer hydrogenation of nitroarenes provides a complementary and straightforward approach to access this class of compound.[3] Unfortunately, there are numerous disadvantages which limit the applications of this approach; these include the need for stoichiometric quantities of earth abundant metal reagent,[4] high catalyst loadings,[5] the

[a] *Dr. S. Doherty, Dr. J. G. Knight, A. A. Alharbi, Dr. C. Wills, Dr. C. Dixon*
Newcastle University Centre for Catalysis (NUCAT), School of Chemistry, Bedson Building, Newcastle University, Newcastle upon Tyne, NE1 7RU (UK)
E-mail: simon.doherty@ncl.ac.uk
julian.knight@ncl.ac.uk

[b] *Dr. C. Cheng*
School of Engineering, Stephenson Building, Newcastle University, Newcastle upon Tyne NE1 7RU (UK)

[c] *Dr. F. Russo Abegão*
School of Engineering, Mertz Court, Newcastle University, Newcastle upon Tyne NE1 7RU (UK)

[d] *Prof. T. W. Chamberlain, H. Yan, A. Griffiths, Prof. R. A. Bourne, Dr. S. M. Collins, Dr. K.-J. Wu*
Institute of Process Research & Development, School of Chemistry and School of Chemical and Process Engineering, University of Leeds, Woodhouse Land, LS2 9JT (UK)
E-mail: t.w.chamberlain@ncl.ac.uk

[e] *Dr. H. Alshaikh.*
Department of Chemistry, Rabigh College of Science and Arts, King Abdulaziz University, Rabigh, Jeddah 21589, Saudi Arabia

Supporting information for this article is available on the WWW under https://doi.org/10.1002/cctc.202400013

© 2024 The Authors. ChemCatChem published by Wiley-VCH GmbH. This is an open access article under the terms of the Creative Commons Attribution License, which permits use, distribution and reproduction in any medium, provided the original work is properly cited.

© 2024 The Authors. ChemCatChem published by Wiley-VCH GmbH

use of toxic reducing agents and/or environmentally harmful additives,[6] poor functional group tolerance,[7] the generation of large amounts of waste and thereby poor atom economy,[8] partial or incomplete reduction to hydroxylamines, hydrazones, azoarenes and azoxyarenes,[9] and contamination of the product with metal. As such, there is considerable interest in developing catalysts that are robust and functional group tolerant and that can operate under mild conditions at low catalyst loadings in environmentally benign solvents and that can be removed and recovered via an operationally straightforward procedure. To this end, Fe/ppmPd nanoparticles and Pd/C in combination with a PEG-containing designer surfactant meet the majority of these criteria by effecting efficient and selective reduction of nitroarenes and heteroarenes under mild conditions in a safe sustainable and environmentally responsible protocol.[10] While a range of homogeneous catalysts also perform this reduction with remarkable efficiency, recovery and reuse of the catalyst can be problematic and expensive ligands are often required to achieve the performance.[11] Alternatively, metal nanoparticles are a promising class of catalyst that has been effective in a wide range of reactions including reductions, oxidations, cross-couplings and cyclisations.[12] While the activity of metal nanoparticle catalysts has been attributed to their high surface area to volume ratios as well as quantum confinement effects,[13] they are inherently unstable with respect to aggregation towards larger species that are less active and/or selective.[14] Thus, for practical applications it is necessary to stabilise metallic nanoparticles for use in catalysis, which is most commonly achieved by impregnation or encapsulation into an organic or inorganic supports[15a–c] such as zeolites,[15d–k] inorganic oxides[15k–o] molecularly modified oxides,[15p–y] Metal Organic Frameworks (MOFs)[15z–ff] porous carbon materials[15gg–oo] or porous organic polymers.[15pp–ddd] To this end, there are a number of recent examples of ruthenium nanoparticle that catalyse the reduction of nitroarenes with promising performance profiles; these include: well-ordered mesoporous silica supported RuNPs,[16a] magnetically separable ruthenium nanoparticles decorated on channelled silica microspheres,[16b] magnetic ruthenium-coated iron nanoparticles,[16c,d] RuNP supported on magnetically separable chitosan,[16e] RuNPs supported on carbon nanotubes[16f–h] or dispersed in a nitrogen doped carbon matrix,[16i] RuNPs immobilized on a ionic liquid-silica conjugate,[16j] and Ru@C60.[16k]

In addition to the site isolation and intrinsic steric stabilisation provided by confinement in these supports, synergistic metal-support interactions between the metal nanoparticles and the encapsulating material can also enhance or modulate the activity, selectivity and stability of the catalyst.[17] For example, platinum nanocrystals modified with $Fe(OH)_x$ catalyse the reduction of 3-nitrostyrene to 3-aminostyrene with remarkable selectivity whereas unmodified PtNPs were much less selective and gave a mixture of 3-aminostyrene, 3-nitro-ethylbenzene and 3-aminoethylbenzene; the high selectivity obtained with $Fe(OH)_x$/Pt was attributed to the Fe^{III}–OH–Pt interfaces which facilitate oxidative coupling of Pt–H species with OH^- to generate a vacancy close to a five coordinate Fe(II) site which captures and reduces the nitro group in preference to the styrene C=C bond because of the oxophilicity of Fe^{2+}.[18] While decoration of high surface area supports with metal binding heteroatom donors has also been used to anchor metallic NPs and hinder their aggregation, heteroatoms have also been reported to have a beneficial effect on activity and selectivity either by regulating the size and shape of the NPs, or through steric confinement by the surface ligands, modification of the surface electronic structure, modulation of the hydrophobic/hydrophilic environment at the surface of the NP and thereby the solubility of the substrate or by facilitating the elementary steps of the catalytic cycle.[19] To this end, phosphine and amine decorated supports[20,21] have been reported to modify the performance of metallic nanoparticles as catalysts for a range of reductions including nitroarenes, carbonyl compounds, arenes and heteroarenes and carbon dioxide as well as the release of hydrogen from formic acid; in the majority of these reports the enhancement in activity or selectivity has been attributed to either the high surface electron density of the nanoparticles or their ultra-small size and effective dispersion. For example, the high activity of PdNPs supported on amine rich silica hollow nanospheres as a catalyst for the hydrogenation of quinoline was attributed to the ultra-small particle size and high surface electron density resulting from coordination of the amine to the nanoparticle surface.[21h] Palladium nanoparticles stabilised by an amino-polymer silica composite, or an amine-modified silica surface were more selective and active for the semi-hydrogenation of alkynes than their unmodified counterparts.[21b,c] and platinum nanoclusters confined in the cavities of UiO-66-NH_2 were markedly more selective as catalysts for the hydrogenation of the C=O bond in cinnamaldehyde than those supported on the external surface of the MOF.[21d,t] Thus, while a large excess of surface coordinating ligand might be expected to have a detrimental effect on activity by blocking active sites and restricting or preventing access of the substrate, these reports provide conclusive evidence that heteroatom donors can have a beneficial influence on catalyst performance.

We have embraced this concept and recently initiated a programme to explore the use of heteroatom donor decorated polymer immobilised ionic liquid stabilised nanoparticles as catalysts for reductions and cross-couplings with the specific aim of systematically investigating the influence of the heteroatom donor on catalyst stability and performance.[22] In particular, we reasoned that the immobilised imidazolium based ionic liquid would stabilise the nanoparticles through weak electrostatic interactions to the surface while the heteroatom donor would coordinate to the surface and provide additional stabilization against aggregation under the conditions of catalysis; as eluded to above the HAD may also enable the surface electronic structure to be modified, the size, morphology and dispersion of the nanoparticles to be controlled or the elementary steps of the catalytic cycle to be facilitated which will allow catalyst properties to be tuned and performance optimised.[23] Moreover, attachment of the ionic liquid and the heteroatom donor to a support would prevent leaching of the ionic liquid, facilitate separation and recovery of the catalyst as well as avoid the use of a large amount of ionic

© 2024 The Authors. ChemCatChem published by Wiley-VCH GmbH

18673899, 2024, 13, Downloaded from https://chemistry-europe.onlinelibrary.wiley.com/doi/10.1002/cctc.202400013 by Imperial College London, Wiley Online Library on [10/09/2025]. See the Terms and Conditions (https://onlinelibrary.wiley.com/terms-and-conditions) on Wiley Online Library for rules of use; OA articles are governed by the applicable Creative Commons License

liquid as the bulk solvent as only a small amount of polymer immobilised ionic liquid is required to stabilize the NPs.

Our preliminary studies in this area have demonstrated that PdNPs stabilised by a phosphine decorated PIIL is a remarkably efficient and selective catalyst for the aqueous phase reduction of the carbon carbon-double bond in α,β-unsaturated carbonyl compounds, the transfer hydrogen of nitroarenes to the corresponding amine and the Suzuki-Miyaura cross-coupling of aryl bromides, while RuNP stabilised by a phosphine oxide decorated PIIL catalyses the selective hydrogenation of aromatic ketones with remarkable efficacy and the hydrolytic release of hydrogen from $NaBH_4$. Most recently we discovered that RuNPs stabilised by a phosphine oxide-decorated PIIL catalyses the selective partial reduction of nitroarenes to the corresponding *N*-arylhydroxylamine as well as complete reduction to the aniline. The increasing number of reports of an enhancement in catalyst performance for nanoparticles stabilized by an amino-modified support has prompted us to extend this program to explore the influence on catalyst efficacy of confinement of RuNPs in a range of amine-decorated large pore ordered mesoporous silica immobilized ionic liquid supports, by varying the density and type of amine donor. Herein we report the characterization of a range of amine-modified Ordered Mesoporous Silica Immobilized Ionic Liquids (OMSIILs) as support for the confinement and stabilization of RuNPs together with a comparative evaluation of their efficacy as catalysts for the aqueous phase reduction of nitroarenes to the corresponding aniline. Our preliminary studies with this class of catalyst revealed a number of interesting features; (i) RuNPs stabilized by amino-modified Ordered Mesoporous Silica Immobilized Ionic Liquids (RuNP@NR_2-OMSIIL) outperform their unmodified counterparts (RuNP@OMSIIL), (ii) the highest TOF to be reported for the partial reduction of nitrobenzene to the corresponding hydrazobenzene using dimethylamine borane as the hydrogen source and (iii) a solvent dependent selectivity when sodium borohydride is used as the hydrogen donor with reactions conducted in ethanol giving high selectivity for the partial reduction to hydrazobenzene while reactions conducted in water, under otherwise identical conditions, gave aniline as the sole product, in the same time. The partial reduction of nitroarenes to the corresponding hydrazoarene is of considerable interest as these products are versatile synthons for the preparation of nonsteroidal anti-inflammatory drugs.[24] Moreover, there are relatively few reports of the selective partial reduction of nitroarenes to the corresponding hydrazoarene,[25] and this is the first example using a ruthenium nanoparticle-based catalyst.

Results and Discussion

Catalyst Synthesis and Characterisation

The ordered mesoporous silica (OMS) COK-12, an analogue of SBA-15, was identified as a suitable support for the immobilization of ionic liquids and modification with amino donors as the synthesis is straightforward and environmentally benign, amenable to modification and the product has large uniform pores.[26] The unmodified COK-12 support **1 a** was prepared in high yield by the room temperature hydrolysis and condensation of sodium silicate in citric acid/sodium citrate buffer using P123 triblock co-polymer surfactant as the structure determining agent (SDA). The ionic liquid and amine decorated COK-12 supports **1 b** and **1 c**–**d**, respectively, were prepared following the same protocol in the presence of 5 mol% of the corresponding imidazolium silica precursor 1,2-dimethyl-3-(3-(triethoxysilyl)propyl)-1*H*-imidazol-3-ium chloride or either triethoxysilylpropylamine or 1-(3-(triethoxysilyl)propyl)pyrrolidine. Similarly, the ionic liquid/amine hybrid COK-12 supports **1 e**–**f** were prepared by conducting the hydrolysis in the presence of a mixture of 5 mol% each of the imidazolium and the associated amine silica precursor (Scheme 1). The surfactant was removed by continuous extraction with ethanol to afford the desired mesoporous silica as a fine off-white powder. Comparison of the FT-IR and MAS ^{13}C NMR spectra of an authentic sample of P123 with the corresponding spectra for **1 a**–**f**, before and after extraction, confirmed that the surfactant had been successfully removed, as evidence by the absence of any resonances between 70–80 ppm characteristic of poly(ethylene oxide)-poly(propylene oxide) co-polymer. The magic angle spinning solid state ^{29}Si spectra of **1 a**–**f** each contain two groups of signals typical for silica; a set of three Q series signals at *ca.* δ 92, 102 and 111 ppm for the tetrasubstituted silicon species $Si(SiO_2)_2(OH)_2$], [$Si(OSi)_3(OH)$] and [$Si(OSi)_4$], respectively, in the inorganic silica framework and a broad ill-defined T-series signal at *ca.* δ 68 ppm associated with the organo-modified silica $RSi(OSi)_3$ (see Figures S6, S11, S17, S23, S28, S34 in the supporting information).[15,27] The disparate intensities of these resonances confirms that these catalysts are comprised mainly of inorganic silicate together with a minor amount of organic silicate resulting from immobilization of the silylated ionic liquid and/or amine on the walls of the mesoporous silica. The ^{13}C CP-MAS spectra of **1 b**–**f**, recorded using the TOSS pulse sequence, contain resonances that are characteristic of the surface attached functionality (see Figures S12, S18, S24, S29, S35 in the support information). For example, the ^{13}C CP-MAS NMR spectrum of **1 b** has two resonances at *ca.* δ 144.6 and δ 122.3 ppm which belong to the C2 and C4/C5 carbon atoms of the imidazolium ring, while signals at δ 7.9 ppm ($SiCH_2$), 22.7 ppm ($CH_2CH_2CH_2$) and 49.6 ppm (CH_2N) are associated with the methylene carbon atoms of the propyl tether connecting the imidazolium ring to the surface;[28] an additional resonance at δ 34.8 ppm is characteristic of the two methyl groups attached to the imidazolium ring. The ^{13}C spectra for supports **1 e**–**f** that also have a surface anchored NH_2 or pyrrolidine each contain a set of signals associated with the methylene groups of the propyl tether. The IR spectra of the silica immobilised ionic liquid **1 b**–**f** and the corresponding catalysts **2 b**–**f** each contain bands at *ca.* 1570 cm^{-1} and 1630 cm^{-1} characteristic of the C=C and C=N stretching vibrations of the imidazolium ring, further confirming that the ionic liquid precursor was incorporated into the COK-12 material (see Figures S7, S13, S19, S25, S30, S36 in the supporting information).[29a–d] The FT-IR spectrum of surface

© 2024 The Authors. ChemCatChem published by Wiley-VCH GmbH

18673899, 2024, 13, Downloaded from https://chemistry-europe.onlinelibrary.wiley.com/doi/10.1002/cctc.202400013 by Imperial College London, Wiley Online Library on [10/09/2025]. See the Terms and Conditions (https://onlinelibrary.wiley.com/terms-and-conditions) on Wiley Online Library for rules of use; OA articles are governed by the applicable Creative Commons License

18673899, 2024, 13, Downloaded from https://chemistry-europe.onlinelibrary.wiley.com/doi/10.1002/cctc.202400013 by Imperial College London, Wiley Online Library on [10/09/2025]. See the Terms and Conditions (https://onlinelibrary.wiley.com/terms-and-conditions) on Wiley Online Library for rules of use; OA articles are governed by the applicable Creative Commons License

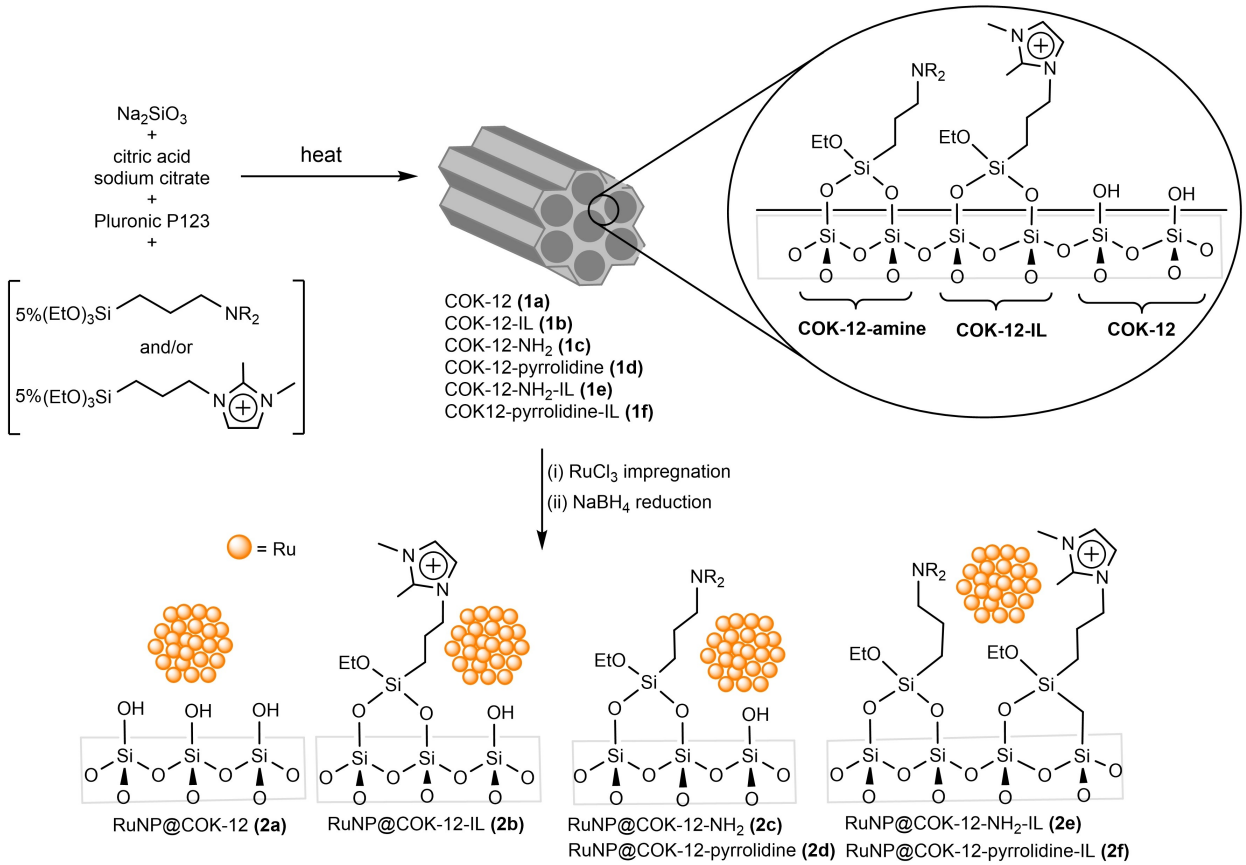

Scheme 1. Synthesis and composition of ordered mesoporous silica COK-12, ionic liquid (IL) and/or amine modified COK-12 (**1 a–f**) and the corresponding RuNP based catalysts **2 a–f**.

modified supports **2 b–f** also contain bands at 2927 cm^{-1} and 2852 cm^{-1} for the symmetric and asymmetric stretching vibrations of the propyl CH_2 groups and a band at *ca.* 1480 cm^{-1} due to the C–N(imidazolium or amine) stretching vibration, which are not present in the spectrum of RuNP@COK-12 (see Figures S40, S50, S60, S70, S80, S90 in the supporting information).[29a–d] The strongest bands at 1071–1054 cm^{-1} and 449 cm^{-1} are associated with the Si–O stretching vibration and the bending vibration of O–Si-O, respectively.[29e–g]

TEM micrographs of **2 a–f** revealed that the ruthenium nanoparticles were near monodisperse with average diameters ranging from 1.6 to 4.5 nm, details of which are provided in the SI; representative micrographs and associated histogram for **2 e**, based on >100 particles, are show in Figure 1 and those for **2 a–d** and **2 f** are presented in the SI (see Figures S44, S54, S65, S74, S84, S94 in the supporting information). Surface characterization of the RuNP-based catalysts **2 a–f** was undertaken by X-ray photoelectron spectroscopy (XPS) with analysis of the Ru 3p regions performed because of overlap of the C 1s with the Ru 3d region. For catalyst **2 a**, where the RuNPs were stabilised by unmodified COK-12, Ru 3p peaks were found at 463.89 eV and 486.15 eV, which were assigned to RuO_2; the presence of RuO_2 species is most likely due to a degree of surface oxidation of the pre-formed metallic ruthenium nanoparticles (Figure 2).[30] For the remaining catalysts **2 b–f**, the $3p_{1/2}$ and $3p_{3/2}$ peak

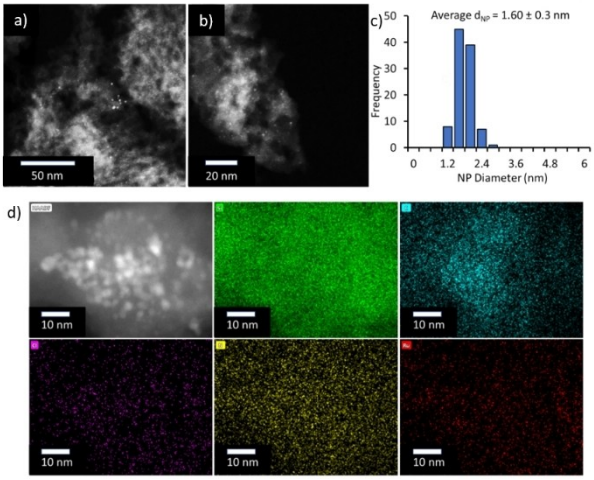

Figure 1. (a-b) High resolution TEM images of **2 e**, (c) the corresponding size distribution determined by counting >100 particles, and (d) HAADF and EDX mapping, showing the distribution of Si (green), C (blue), Cl (purple), N (yellow) and Ru (red).

positions appeared at lower binding energies of 484.18–485.09 eV and 461.78–462.78 eV, respectively, which are closer to the regions reported for metallic ruthenium; the $3d_{3/2}$ and $3d_{5/2}$ binding energies of 283.76–286.95 eV and 280.57–

© 2024 The Authors. ChemCatChem published by Wiley-VCH GmbH

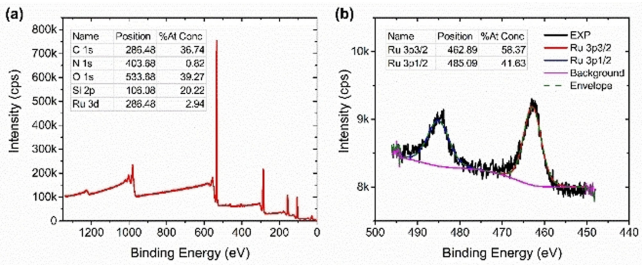

Figure 2. XPS data showing (a) the overall survey scan and (b) the Ru 3p region of amino-modified ordered mesoporous silica immobilized ionic liquid-stabilised ruthenium nanoparticles **2 e**.

281.70 eV, respectively, also support this assignment (see Figures S45–46, S56–57, S66–67, S76–77, S86–87, S96–97 in the supporting information). The porosity and surface area of the modified COK-12 supports **1 a–f** was analysed by N_2 adsorption-desorption isotherms at 77 K, and all samples showed characteristic type IV curves and H1-type hysteresis loops in the relative pressure (p/p_0) range of 0.45–0.80 which are consistent with a highly ordered mesoporous material (see Figures S9, S15, S21, S32, S38 in the supporting information). The BET surface area (S_{Bet}), pore volume (V_p) and average pore diameter (d) for COK-12 (**1 a**) are 726 $m^2 g^{-1}$, 0.67 $cm^3 g^{-1}$ and 5.48 nm, respectively. For comparison, the BET surface area of 467 $m^2 g^{-1}$ and pore volume of 0.45 $cm^3 g^{-1}$ reported for COK-12 are lower.[26] The surface area of supports **1 b–f** (446–643 $m^2 g^{-1}$) are markedly lower than that for the unmodified COK-12, consistent with modification of the surface with organoamine and/or imidazolium groups in the mesoporous channels.[15p,w,x,21q] As expected, immobilisation of the RuNPs onsupports **2 a–f** resulted in a decrease in the BET surface area to 517 $m^2 g^{-1}$ for **2 a** and 213–269 $m^2 g^{-1}$ for **2 b–f**, which corresponds to a reduction of *ca.* 200 $m^2 g^{-1}$, (see Figures S43, S52, S62, S72, S88, S92 in the supporting information) indicating that the RuNPs may block some of the smaller pores and thereby reduce access (Table S2 in the supporting information). The amount of accessible amine on **1 c–f** of 0.61–0.67 mmol g^{-1} was determined following a literature titration protocol[31] and is close to the theoretical values of 0.73–0.80 mmol g^{-1}. The amount of accessible amine on catalysts **2 c-f** was determined to be 0.55–0.64 mmol g^{-1} which corresponds to amine/ruthenium ratios between 1.6 and 6.1. Thermogravimetric analysis of supports **1 a–f** show loss of solvent between 50 °C and 100 °C while further mass loss of 25–30 % due to decomposition occurs at *ca.* 200–220 °C (see Figures S8, S14, S20, S26, S31, S37). For comparison, catalysts **2 a–f** appear to decompose closer to 180 °C, which is well below the temperatures required for the reduction of nitrobenzene (see Figures S41, S51, S61, S71, S81, S91).

RuNP@OMSIIL Catalysed Reduction of Nitroarenes

The catalytic reduction of nitroarenes was initially targeted to compare the efficacy of **2 e** against other noble metal nanoparticle catalysts as well as RuNPs stabilized by PIIL which were recently shown to be a remarkably efficient and selective catalyst for the partial reduction of nitroarenes to *N*-arylhydroxylamines.[22] A series of catalytic reductions were first conducted with nitrobenzene as the benchmark substrate as this reduction has been catalyzed by RuNPs stabilized by various supports including PVP,[32a–c] bulky amphiphilic PEG-modified tripodal ligands,[32d] dendrimers,[32e,f] polystyrene,[32g] carbon nanotubes,[16f] polystyrene,[32h] TiO_2,[32i] and phosphine-functionalized ionic liquids.[20b,c] Initial exploratory reactions investigated the effect of the reducing agent, time, temperature and solvent on conversion and selectivity, full details of which are presented in Table 1. A preliminary reduction conducted in ethanol at 70 °C under nitrogen using 0.5 mol% **2 e** as the catalyst and four mole equivalents of sodium borohydride gave complete conversion with 94 % selectivity for aniline after 16 h. Under these conditions hydrazobenzene was identified as the only other major species (5 %) together with a trace amount of azobenzene, which most likely resulted from serendipitous oxidation of the hydrazobenzene during work-up (Table 1, entry 1).

Interestingly, when the reaction time was reduced to 1 h the nitrobenzene was also completely consumed but hydrazobenzene was obtained as the major product in 96 % selectivity (Table 1, entry 2), together with a minor amount of *N*-phenylhydroxylamine (2%) and azoxybenzene (1 %). Such a high selectivity for hydrazobenzene is quite remarkable as a survey of the literature revealed that there are only a handful of reports of the selective partial reduction of nitroarenes to the corresponding hydrazoarene. Recent examples include a nickel–tungsten carbide composite nano catalyst with hydrazine hydrate,[25a] gold nanoparticles supported on hexagonal boron nitride nanoplates with isopropanol/KOH,[25b] indium tribromide and a hydrosilane,[25c] polystyrene supported gold nanoparticles,[25d] and electrochemical reduction with gaseous ammonia.[25e] Thus, this is the first example of the selective partial reduction of nitrobenzene to hydrazobenzene using a ruthenium nanoparticle-based catalyst and, moreover, the initial TOF of 320 mol nitrobenzene converted mol Ru^{-1} h^{-1} appears to be higher than the systems described above. While hydrazoarenes have also recently been prepared via a tandem selective reduction of nitroarenes, the sequence involved reduction of the nitroarene to the *N*-arylhydroxylamine subsequent oxidation to the azoxyarene followed by reduction to the corresponding hydrazoarene,[33] the protocol described herein is potentially more straightforward and practical. The presence of a large amount of hydrazobenzene at short reaction times is consistent with reduction *via* the condensation pathway (Scheme 2).[4] In stark contrast, when the reduction of nitrobenzene was conducted in water for 1 h, under otherwise identical conditions, the conversion reached 97 % but gave aniline as the only product with no evidence for azo-based intermediates i.e. the solvent either has a dramatic influence on the kinetics of this multistep reduction, in this case the reduction of hydrazobenzene to aniline, or it switches the pathway for reduction from condensation to form azo intermediates to direct reduction via the *N*-arylhydroxylamine

© 2024 The Authors. ChemCatChem published by Wiley-VCH GmbH

18673899, 2024, 13, Downloaded from https://chemistry-europe.onlinelibrary.wiley.com/doi/10.1002/cctc.202400013 by Imperial College London, Wiley Online Library on [10/09/2025]. See the Terms and Conditions (https://onlinelibrary.wiley.com/terms-and-conditions) on Wiley Online Library for rules of use; OA articles are governed by the applicable Creative Commons License

Table 1. Ruthenium nanoparticle catalysed reduction of nitrobenzene as a function of solvent, temperature, hydrogen donor and catalyst.[a]

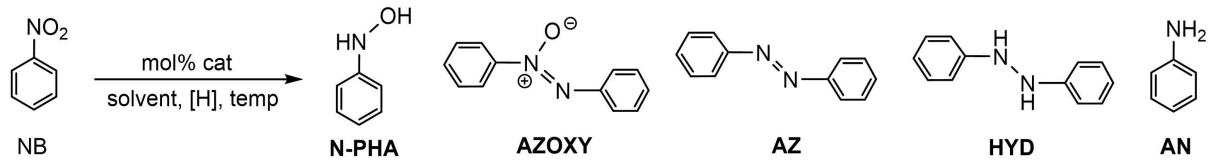

Entry	Catalyst	Hydride (equiv.)	Temp (°C)	Solvent	Time (h)	Conv (%)[b]	(%) Selectivity[c] AN	N-PHA	AZOXY	AZ	HYD
1	**2e** (0.5)	$NaBH_4$ (4)	70	EtOH	16	100	100	0	0	0	0
2	**2e** (0.5)	$NaBH_4$ (4)	70	EtOH	1	99	96	2	1	0	0
3	**2e** (0.5)	$NaBH_4$ (4)	70	H_2O	1	97	100	0	0	0	0
4	**2e** (0.5)	DMAB (4)	70	EtOH	3	86	100	0	0	0	0
5	**2e** (0.5)	N_2H_4 (4)	70	EtOH	3	2	0	0	100	0	0
6	**2e** (0.5)	HCO_2NH_4	70	EtOH	3	70	94	3	3	0	0
7	**2e** (0.5)	HCO_2H (4)	70	EtOH	3	3	0	67	33	0	0
8	**2e** (0.25)	DMAB (4)	70	EtOH	3	74	100	0	0	0	0
9	**2e** (0.1)	DMAB (4)	70	EtOH	3	38	98	1	1	0	0
10	**2e** (0.05)	DAMB (4)	70	EtOH	3	16	97	1	2	0	0
11	**2e** (0.5)	DMAB (4)	70	H_2O	3	100	100	0	0	0	0
12	**2e** (0.5)	DMAB (4)	70	EtOH/H_2O	3	80	93	4	3	0	0
13	**2e** (0.5)	DMAB (4)	70	Toluene	3	25	77	1	22	0	0
14	**2e** (0.5)	DMAB (4)	70	2-MeTHF	3	12	82	0	18	0	0
15	**2e** (0.5)	DMAB (4)	70	PC	3	22	68	0	32	0	0
16	**2e** (0.5)	DMAB (4)	70	H_2O	1.5	100	99	0	0	0	0
17	**2e** (0.5)	DMAB (4)	60	H_2O	1.5	100	>99	0	0	0	0
18	**2e** (0.5)	DMAB (4)	50	H_2O	1.5	98	>99	0	0	0	0
19	**2e** (0.5)	DMAB (3)	50	H_2O	1.5	56	92	0	8	0	0
20	**2e** (0.5)	DMAB (2)	50	H_2O	1.5	45	96	0	4	0	0
21	**2a** (0.5)	DMAB (4)	50	H_2O	1.5	36	68	21	11	0	0
22	**2b** (0.5)	DMAB (4)	50	H_2O	1.5	76	98	0	2	0	0
23	**2c** (0.5)	DMAB (4)	50	H_2O	1.5	91	96	3	1	0	0
24	**2d** (0.5)	DMAB (4)	50	H_2O	1.5	48	95	0	5	0	0
25	**2f** (0.5)	DMAB (4)	50	H_2O	1.5	67	94	3	3	0	0

[a] Reaction conditions: Conducted under nitrogen, 1.0 mmol nitrobenzene, mol% catalyst, 1 mL solvent, hydride source, time, temperature. [b] % Conversion determined by ^{1}H NMR spectroscopy using 1,4-dioxane as internal standard. Average of at least three runs. [c] Selectivity for aniline [% AN / (% *N*-PHA + % AZOXY + % AZ + % HYD + % AN)]×100%. [d] Selectivity for hydrazobenzene [% HYD / (% *N*-PHA + % AZOXY + % AZ + % HYD + % AN)]×100%.

(Scheme 2).[34] To this end, there have been several recent reports of solvent dependent selective reduction of nitroarenes including, $InBr_3/Et_3SiH$ which gave the azoxyarene in THF and the hydrazoarene in DMF,[25c] an electrochemical reduction of nitroarenes with gaseous ammonia which gave azoxy, azo and hydrazo compounds depending in the cell voltage and solvent,[25e] and a RuNP/CN catalyzed hydrazine hydrate-mediated reduction of nitroarenes which gave the *N*-arylhydoxylamine in THF and the arylamine in water.[16f] Studies are currently underway to explore the kinetics of each fundamental step of this reduction as a function of the solvent and hydrogen donor and to investigate the selectivity as a function of the catalyst-support composition to develop a more detailed understanding of the factors that influence catalyst performance and inform the rational design of more selective catalysts.

Interested in exploring the solvent dependent selective formation of hydrazobenzene in ethanol compared with rapid and near quantitative formation of aniline in water, the conversion and composition for the $NaBH_4$-mediated reduction of nitrobenzene was monitored as a function of time in both solvents at 70 °C using 0.5 mol% **2e** as the catalyst. The composition-time profile in ethanol (Figure 3a), obtained by conducting a series of parallel reactions for different times, shows that nitrobenzene is completely consumed within 30 min during which time hydrazobenzene is formed as the major species (96%) together with minor amounts of azoxybenzene and azobenzene, consistent with our preliminary experiments

© 2024 The Authors. ChemCatChem published by Wiley-VCH GmbH

18673899, 2024, 13, Downloaded from https://chemistry-europe.onlinelibrary.wiley.com/doi/10.1002/cctc.202400013 by Imperial College London, Wiley Online Library on [10/09/2025]. See the Terms and Conditions (https://onlinelibrary.wiley.com/terms-and-conditions) on Wiley Online Library for rules of use; OA articles are governed by the applicable Creative Commons License

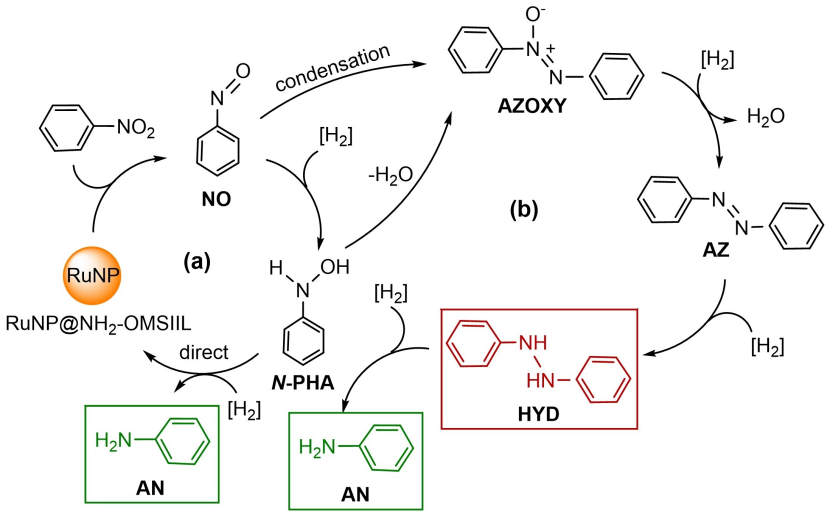

Scheme 2. General mechanisms (Haber) for the reduction of nitroarenes (a) direct pathway (b) condensation pathway, highlighting the selective partial reduction to hydrazobenzene (red) and complete reduction to aniline (green) achieved with RuNP@NH_2-OMSIIL (**2 e**)

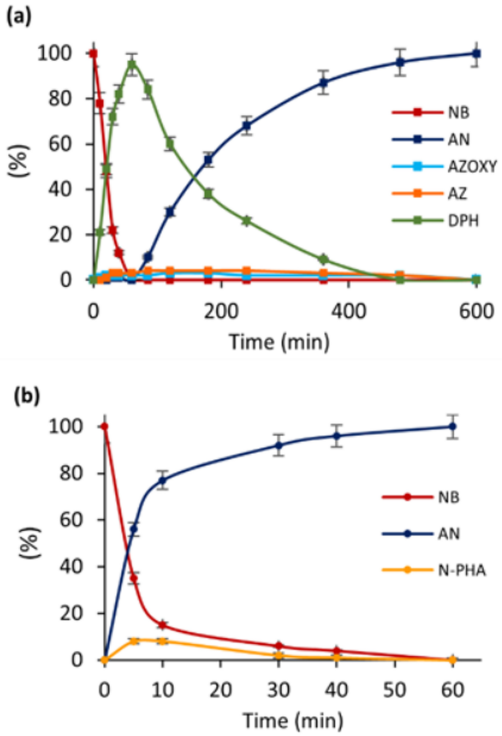

Figure 3. (a) Composition-time profile for the sodium borohydride-mediated reduction of nitrobenzene (NB) in ethanol at 70 °C under nitrogen catalyzed by 0.5 mol% **2 e**. (b) Composition-time profile for the sodium borohydride-mediated reduction of nitrobenzene (NB) in water at 70 °C under nitrogen catalyzed by 0.5 mol% **2 e**.

describe above. Longer reaction times resulted in gradual consumption of the hydrazobenzene to afford aniline, which was obtained as the sole product after 10 h. In contrast, the corresponding composition time profile in water (Figure 3b) shows rapid consumption of nitrobenzene with concomitant formation of aniline in the early stages of the reaction together with a build-up of *N*-phenylhydroxylamine which reached a maximum concentration after 8 min; this was gradually consumed, and aniline was formed as the sole product after 60 minutes. Thus, while the profile in ethanol is consistent with reduction via condensation and the generation of azo and azoxy species, the reduction in water appears to occur via the direct pathway involving rapid reduction of the *N*-phenylhydroxylamine, however, we cannot unequivocally rule out condensation with facile reduction of the azo-based intermediates (Scheme 2).[34]

Having identified conditions for the highly selective partial reduction of nitrobenzene to hydrazobenzene, the protocol was applied to the reduction of a selection of substituted nitroarenes to assess the scope and efficacy of **2 e**. These reactions were conducted in ethanol at 70 °C, using 0.5 mol% **2 e** and four equivalents of $NaBH_4$ as the hydrogen donor and reaction times were varied to obtain the best compromise of selectivity and conversion; full details of which are provided in Table 2. Gratifyingly, high conversions were obtained with nitroarenes substituted with electron withdrawing groups such as 4-chloronitrobenzene and 4-bromonitroarenes which were reduced to the corresponding hydrazoarene with 88 % and 75 % selectivity, respectively, with no evidence for competing hydrodehalogenation to afford either nitrobenzene or hydrazobenzene; in each case the only other identifiable species was the fully reduced aniline. Similarly, a high conversion and complete selectivity was also obtained with 4-nitrobenzonitrile which reached 91 % conversion to afford 4,4′-dicyanohydrazobenzene as the only detectable product after 5 h; interestingly though, when the reaction time was reduced to 1 h the corresponding azo compound, 4,4′-(diazene-1,2-diyl)dibenzonitrile, was obtained as the major product with 86 % selectivity at complete conversion. Under the same conditions, the reduction of 4-nitrobenzotrifluoride reached complete conversion after 5 h to afford the corresponding hydrazoarene in 81 % selectivity, together with minor amounts of the 4-(trifluoromethyl)aniline (11 %) and the *N*-(4-(trifluoromethyl)phenyl)hydroxylamine (8 %)

© 2024 The Authors. ChemCatChem published by Wiley-VCH GmbH

18673899, 2024, 13, Downloaded from https://chemistry-europe.onlinelibrary.wiley.com/doi/10.1002/cctc.202400013 by Imperial College London, Wiley Online Library on [10/09/2025]. See the Terms and Conditions (https://onlinelibrary.wiley.com/terms-and-conditions) on Wiley Online Library for rules of use; OA articles are governed by the applicable Creative Commons License

Table 2. Partial reduction of nitroarenes to the corresponding hydrazoarene with $NaBH_4$ in ethanol catalyzed by RuNP@NH_2-OMSIIL (**2 e**).[a]

Product	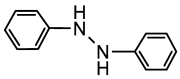	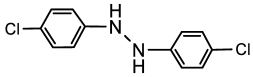	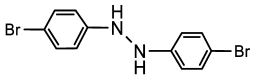
Conversion[b]/Yield[c]	100%/92% (1 h)	98%/91% (40 min)	100%/83% (3 h)
Selectivity[d]	96%	88%	75%
Product	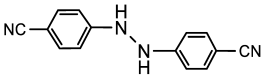	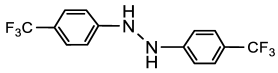	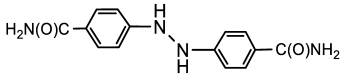
Conversion[b]/Yield[c]	91%/82% (5 h)	100%/87% (5 h)	81%/69% (90 min)
Selectivity[d]	100%	81%	100%

[a] Reaction conditions: Conducted under nitrogen, 1.0 mmol nitroarene, 0.5 mol% **2 e**, 1 mL ethanol, 4 mmol $NaBH_4$, time, 70 °C. [b] % Conversion determined by ^{1}H NMR spectroscopy using 1,4-dioxane as internal standard, reaction time in brackets. Average of at least three runs. [c] Yield determined from the selectivity and the mass of isolated material after aqueous workup. [d] Selectivity for hydrazoarene [% HYD / (% *N*-PHA + % AZOXY + % AZ + % HYD + % AN)]×100%.

while 4-nitrobenzamide was reduced with complete selectivity for the hydrazoarene, 4,4′-(hydrazine-1,2-diyl)dibenzamide, at 81% conversion after 90 min. In contrast, the reduction of nitroarenes bearing electron donating groups such as 4-nitroanisole, 4-nitroaniline and *N,N*-dimethyl-4-nitroaniline all gave the corresponding amine as the major product and only minor amounts of the hydrazoarene were observed, which suggests that reduction of electron rich intermediates is extremely facile under these conditions or that the reduction of this class of substrate occurs via the direct pathway.

Variation of the hydrogen donor revealed that the use of dimethylamine borane (DMAB) resulted in 86% conversion to aniline as the sole product when the reaction was conducted in ethanol at 70 °C for 3 h (Table 1, entry 4); this is in stark contrast to the high selectivity for hydrazobenzene obtained with $NaBH_4$ in ethanol under otherwise identical conditions and further highlights that the selectivity of this reduction depends on a combination of factors including the solvent, reducing agent as well as the catalyst and its support. While hydrazine hydrate has been reported to be the optimum hydrogen donorfor the selective catalytic reduction of nitroarenes with nanoparticles including polystyrene supported IrNPs, RuNPs and RuCoNPs,[32h,35a,b] RuNP/CNT nanohybrids,[16f] PdNP/carbon nitride,[35c] PdNP immobilized on carbon nanospheres,[35d] PdAuNPs/TiO_2,[35e] and solid supported PtNPs,[35f] a reduction of nitrobenzene using 0.5 mol% **2 e** and 4 equivalents of hydrazine hydrate only reached 5% conversion to azoxybenzene as the sole product after 16 h. Other common reducing agents such as sodium formate, formic acid and formic acid triethylamine azeotrope gave either negligible or low conversions under the same conditions (Table 1, entries 5–7). The high conversion obtained with DMAB after only 3 h prompted us to conduct further optimization studies with this reducing agent.

A brief survey of the catalyst loading confirmed that the optimum conversion and selectivity for aniline was achieved with 0.5 mol% **2 e** as a reduction in the catalyst loading to 0.25 mol% resulted in a concomitant reduction in conversion to 74% after 3 h, albeit with >99% selectivity for aniline; the conversion decreased further to 38% and then to 16% when the catalyst loading was reduced to 0.1 and 0.05 mol%, respectively (Table 1, entries 8–10). While complete conversion to aniline could be obtained by increasing the catalyst loading to 1 mol%, the high conversion and complete selectivity for aniline obtained with 0.5 mol% prompted us to conduct further catalytic studies and substrate screening with this loading. As the nanoparticle catalyzed reduction of nitroarenes has been reported to be solvent dependent,[16f,35a,36a–c] the efficacy of **2 e** as a catalyst for the reduction of nitrobenzene was examined in a selected range of common solvents. Table 1 reveals that reductions conducted in water reached quantitative conversion with 100% selectivity for aniline after only 3 h, whereas the use of a 1:1 mixture of ethanol and water under otherwise identical conditions gave 80% conversion to a mixture of azoxybenzene and aniline (Table 1, entries 11–12). Markedly lower conversions and selectivities for aniline were obtained under the same conditions in toluene, 2-Me-THF and propylene carbonate (Table 1, entries 13–15); the low selectivity for aniline in these solvents was due to incomplete reduction to azoxybenzene. Thus, water was identified as the preferred solvent based on the short reaction time required to reach high conversion with complete selectivity for aniline as well as its green and environmentally benign properties, the practical advantages for isolating the product and the potential benefits associated with the hydrophobic effect such as faster reaction rates and greater selectivities compared to those obtained in organic solvent-based systems.[37]

As complete conversion was obtained for the reduction of nitrobenzene at 70 °C with 0.5 mol% even when the reaction time was reduced to 1.5 h (Table 1, entry 16), the influence of the temperature on conversion and selectivity was investigated to identify an optimum temperature to achieve high conversion to aniline. While quantitative conversion to aniline was also obtained after 1.5 h when the temperature was lowered to 60 °C, a further reduction in the reaction temperature to 50 °C gave 98% conversion with >99% selectivity for aniline at the same time (Table 1, entries 17–18). A study of the conversion and selectivity profile as a function of the DMAB to nitrobenzene mole ratio was also conducted to establish the

© 2024 The Authors. ChemCatChem published by Wiley-VCH GmbH

18673899, 2024, 13, Downloaded from https://chemistry-europe.onlinelibrary.wiley.com/doi/10.1002/cctc.202400013 by Imperial College London, Wiley Online Library on [10/09/2025]. See the Terms and Conditions (https://onlinelibrary.wiley.com/terms-and-conditions) on Wiley Online Library for rules of use; OA articles are governed by the applicable Creative Commons License

optimum amount of reducing agent to achieve high conversion to aniline. The conversion dropped quite dramatically from 98% after 1.5 h with four equivalents of DMAB to 56% with three equivalents and 45% with two equivalents under otherwise identical conditions (Table 1, entries 19–20). This drop in conversion was accompanied by a decrease in selectivity due to incomplete reduction to intermediates such as azoxybenzene and *N*-phenylhydroxylamine. An increase in the DMAB to nitrobenzene mole ratio from 4 to 20 revealed that the initial rate, as measured by the TOF at *ca.* 20% conversion, increased from 210 mol nitrobenzene converted mol Ru^{-1} h^{-1} to 320 mol nitrobenzene converted mol Ru^{-1} h^{-1} and ultimately reached a plateau at 335 mol nitrobenzene converted mol Ru^{-1} h^{-1} for a ratio of 25, above which the reaction kinetics were independent of the DMAB concentration (Figure S1 in the supporting Information). Even though the optimum rate was obtained with a DMAB to nitrobenzene ratio of *ca.* 25, further studies and substrate screening were conducted with four mole equivalents of DMAB since near quantitative conversion and complete selectivity for aniline could be obtained after only 1.5 h and the use of only a slight excess of reducing agent improves the reagent efficiency of the process, which will be crucial for scale-up. To this end, a preliminary scale-up reaction for the reduction of nitrobenzene (10 mmol) in water using a catalyst loading of 0.05 mol% and 4 mole equivalents of DMAB reached 95% conversion with 91% selectivity for aniline after 24 h at 60 °C, which corresponds to a TON of 1,900. Following a study by Dimitratos,[15o] the influence of the stirring speed on the initial TOF for the reduction of nitrobenzene catalysed by 0.5 mol% **2e** with 4 equivalents of DMAB at 50 °C was explored to map the region in which the rate is mass transfer limited. Not surprisingly, the rate increased as the stirring speed increased from 100 to 600 rpm after which the initial rate appeared to reach a plateau indicating that reactions conducted above this stirring speed are under kinetic control (Figure S2 in the supporting information). Finally, a background control reaction for the DMAB mediated reduction of nitrobenzene with three equivalents of reducing agent conducted in the presence of the COK-12 support **1e** but in the absence of catalyst gave no conversion after 3 h at 70 °C which confirmed that the RuNPs were necessary for the reduction.

Having identified optimum conditions for the DMAB-mediated reduction of nitrobenzene to aniline, the conversion and composition of a reaction was mapped as a function of time in water at 50 °C. The data in Figure 4, obtained by quenching a series of parallel reactions at different times and quantifying the composition by ^{1}H NMR spectroscopy, shows that the nitrobenzene is consumed with concomitant formation of aniline and the accumulation of a trace amount of *N*-phenylhydroxylamine. As described above for the sodium borohydride mediated reduction of nitrobenzene in water using **2e** as the catalyst, this profile is consistent with reaction via the direct pathway as there was no evidence for any azo-based products, although the condensation pathway cannot be unequivocally ruled out as the reduction of each intermediate may be extremely rapid.

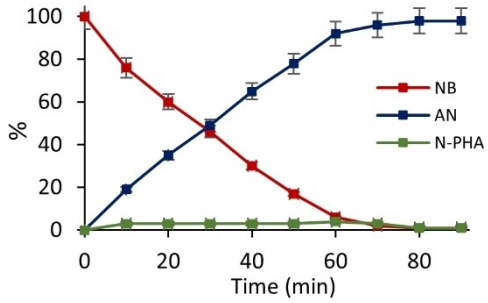

Figure 4. Composition-time profile for the dimethylamine borane-mediated reduction of nitrobenzene (NB) in water at 50 °C under nitrogen, catalyzed by 0.5 mol% **2e**.

Finally, the influence on catalyst performance of the various components *i.e.* the immobilised ionic liquid, the amine and the IL/amine combination was examined by exploring the conversion as a function of catalysts **2a–f**, under the standard conditions identified above. The conversion of 36% obtained with catalyst supported on unmodified COK-12 (**2a**) shows that modification with either an ionic liquid or an amine resulted in a significant improvement in activity as **2b** and **2c** gave 76% and 91% conversion, respectively (Table 1 entries 21–23). The data in Table 1 also reveals that modification of COK-12 with a protic amine resulted in a greater improvement in performance than modification with a tertiary amine as catalyst **2d** only gave 48% conversion, albeit with 95% selectivity (Table 1, entry 24). Finally, it is also clear that COK-12 decorated with a protic amine and an ionic liquid affords the most efficient catalyst as a reduction using 0.5 mol% **2e** reached 98% conversion with >99% selectivity; in comparison its pyrrolidine-ionic liquid modified counterpart **2f** only reached 67% conversion with 94% selectivity at the same time, which underpins the beneficial role of the protic amine (Table 1, entry 25). While modification of COK-12 with the amine and the imidazolium results in a significant improvement in catalyst performance, at this stage it is not possible to determine whether the amine and/or ionic liquid influences both the size of the NPs and their performance profile or whether the size of the NPs is responsible for the changes in performance. Moreover, as **2c–f** each have a different ruthenium/amine ratio it is also not clear how this factor impacts performance. Thus, future studies will explore the influence of the amine to ruthenium and imidazolium to ruthenium ratios on the growth of the nanoparticles and/or their selectivity and activity profiles to deconvolute the factors that control catalyst performance. This will be achieved by systemically varying the loading of the amine and/or the imidazolium on RuNP@COK-12-NH_2-Im, preparing catalysts with a range of ruthenium loadings and conducting a detailed study of their efficacy to establish a composition performance relationship. To this end, there are an increasing number of reports in which molecular modification of a surface has been shown to control the efficiency of nanoparticle-based catalysts for hydrogenation, hydrodeoxygenation and hydrogenolysis reactions;[15p–x] as such it will be crucial to develop an understanding of how surface modifica-

© 2024 The Authors. ChemCatChem published by Wiley-VCH GmbH

18673899, 2024, 13, Downloaded from https://chemistry-europe.onlinelibrary.wiley.com/doi/10.1002/cctc.202400013 by Imperial College London, Wiley Online Library on [10/09/2025]. See the Terms and Conditions (https://onlinelibrary.wiley.com/terms-and-conditions) on Wiley Online Library for rules of use; OA articles are governed by the applicable Creative Commons License

tion affects NP synthesis and performance to enable the rational design of more efficient systems.

The heterogeneous nature of **2e** was investigated by performing a hot filtration experiment which involved conducting two reactions in parallel at 50 °C using 0.5 mol% **2e** and four equivalents of DMAB to catalyse the reduction of nitrobenzene. One of the reaction mixtures was left for 3 h to provide a benchmark for comparison while the other was filtered through a 45 μm syringe filter after 30 min, when it had reached *ca.* 50 % conversion; the composition of this filtrate was then monitored as a function of time for a further 90 min. The resulting composition-time profile in Figure 5 clearly shows that the filtration quenched the reduction as there was no further measurable change in conversion, indicating that the active species had been removed and that the catalyst is either heterogeneous or that any leached catalyst is much less active or inactive. Analysis of the organic filtrate collected after the filtration revealed that the ruthenium content was below the detection limit of the ICP-OES suggesting that the catalyst is most likely heterogeneous, and that leaching to generate species that are less active is not significant. However, this analysis does not enable us to distinguish a pathway that involves a leaching and re-deposition process. A complementary hot filtration experiment was also conducted in which a reduction was allowed to reach complete conversion before being filtered through a 45 μm syringe filter, an additional portion of nitrobenzene was then added to the filtrate and the composition of the reaction mixture monitored. Even after 2 h the composition-time profile showed no further conversion of nitrobenzene confirming that filtration had removed the active species.

The stability of **2e** as a catalyst for the dimethylamine borane-mediated reduction of nitrobenzene to aniline was also investigated by monitoring the conversion and selectivity profile as a function of reuse. The reuse study was conducted by monitoring the activity and selectivity profile for the dimethylamine borane mediated reduction of nitrobenzene in water for 1 h to ensure that reactions did not reach complete conversion to enable any changes in the activity and selectivity to be detected. After 1 h an additional portion of substrate was added together with a further 4 equivalents of DMAB and the profile monitored for another 1 h; this sequence was repeated across three runs to explore the efficiency of **2e** as a function of reaction time and reuse number. The data illustrated in Figure 6a shows a slight drop in the activity after the first run with a more significant reduction in activity and a drop in selectivity after the second run as the reaction only reached 61 % conversion to afford a mixture of aniline (83 %) and *N*-phenylhydroxylamine (17 %) after 1 h; a similar selectivity profile was obtained in the fourth run albeit with a slightly lower conversion than that for run 3. However, complete conversion to aniline could still be obtained by increasing the reaction time to 3 h. ICP-OES analysis of the organic phase collected after all

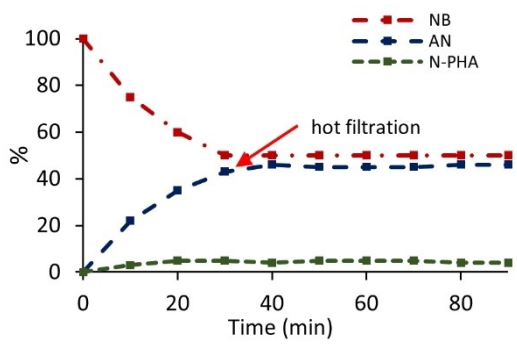

Figure 5. Hot filtration experiment for the dimethylamine borane-mediated transfer hydrogenation of nitrobenzene (NB) in water at 50 °C catalyzed by 0.5 mol% **2e** showing that the reduction is completely quenched after filtration at t = 35 min. [Red line – composition of nitrobenzene (NB), blue line – composition of aniline (AN) and green line – composition of N-phenylhydroxylamine (N-PHA)].

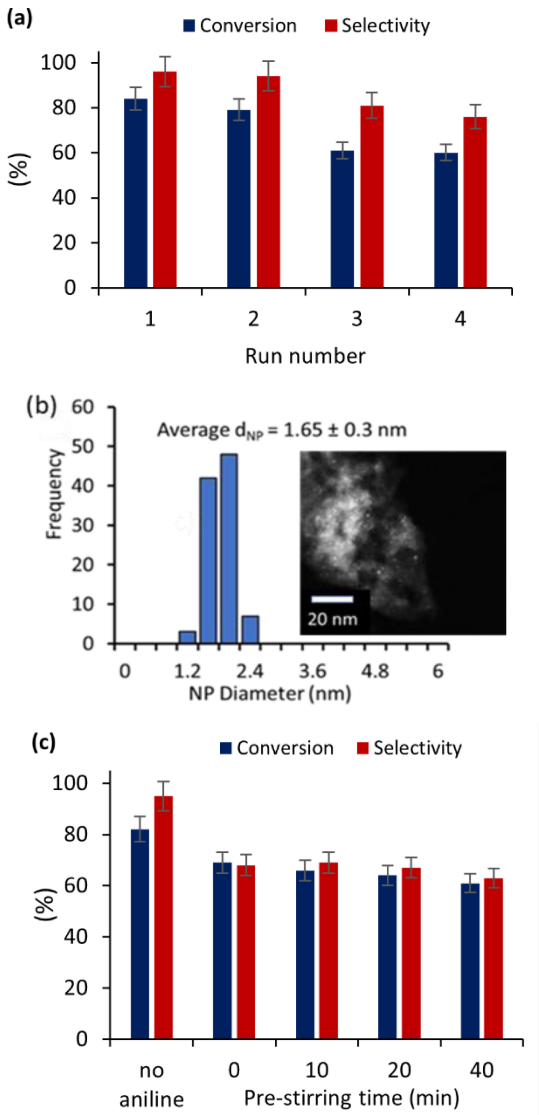

Figure 6. (a) Recycle study for the dimethylamine borane-mediated reduction of nitrobenzene conducted in water at 50 °C and catalysed by 0.5 mol% **2e**. (b) sizing histogram of RuNPs for **2e** after four runs and a TEM image of the recovered material revealing an average NP diameter of 1.65 ± 0.3 nm (c) Conversion and selectivity as a function of aniline pre-stirring time for the DMAB-mediated reduction of nitrobenzene in water at 50 °C catalysed by 0.5 mol% **2e**. Blue bars - conversion of nitrobenzene and red bars - selectivity for aniline.

© 2024 The Authors. ChemCatChem published by Wiley-VCH GmbH

18673899, 2024, 13, Downloaded from https://chemistry-europe.onlinelibrary.wiley.com/doi/10.1002/cctc.202400013 by Imperial College London, Wiley Online Library on [10/09/2025]. See the Terms and Conditions (https://onlinelibrary.wiley.com/terms-and-conditions) on Wiley Online Library for rules of use; OA articles are governed by the applicable Creative Commons License

four runs revealed that only 1.4% of the ruthenium had leached and such a small amount of leaching would not account for the drop in conversion. TEM analysis of the catalyst sample recovered after the 4th run showed that the RuNPs remained monodisperse with no significant change in size and distribution as the mean diameter of 1.65±0.3 nm is similar to that of 1.60±0.3 nm for a freshly prepared sample of **2e** (Figure 6b). As the drop in conversion after the first run did not appear to be due to leaching or excessive aggregation, a poisoning experiment was conducted to explore whether the passivation could be caused by coordination of the aniline product to the active surface ruthenium sites as this could either prevent access of the substrate or modify the catalytic activity/selectivity. Poisoning was explored by pre-stirring an aqueous suspension of catalyst **2e** with 100 equivalents of aniline at 50 °C for a range of pre-stirring times prior to adding the substrate and 4 equivalents of DMAB to assess whether the nitrogen donor of the product influences its performance profile. Reductions conducted for 1 h after pre-stirring the catalyst with aniline for 0 min, 10 min, 20 min and 40 min resulted in a drop in conversion from 82% to *ca.* 61%, together with a concomitant decrease in the selectivity for aniline due to the formation of *N*-phenylhydroxylamine (Figure 6c), suggesting that the aniline that accumulates during successive reuses modifies the activity and selectivity profile of the catalyst. While further studies are required to establish the origin of this change in selectivity, we note that there have been numerous reports of the use of an amine additive to improve selectivity for *N*-arylhydroxylamine in the reduction of nitroarenes. For example, high selectivity for the partial hydrogenation of nitrobenzene to *N*-phenylhydroxylamine has been achieved under mild conditions using ethylenediamine as a modifier for platinum nanowires whereas the use of unmodified commercial platinum black favoured complete reduction to afford aniline as the main product.[38a] Similarly, the use of *N,N,N′,N′*-tetramethylethylenediamine as an additive for platinum nanoparticles supported on active carbon (NanoSelect™) improved its selectivity as a catalyst for the hydrogenation of nitroarenes to the corresponding *N*-arylhydroxylamine,[35c] while the addition of an amine to commercial platinum on silica poisoned with DMSO also resulted in a significant enhancement in yield and selectivity for *N*-phenylhydroxylamine with primary amines giving the highest selectivities.[38b] Nitrogen adsorption studies on catalyst **2e** recovered from a scale-up recycle experiment revealed only a slight change in the textural properties with a minimal increase in the BET surface area from 227 $m^2 g^{-1}$ to 246 $m^2 g^{-1}$ and the pore volume from 0.589 $cm^3 g^{-1}$ to 0.609 $cm^3 g^{-1}$. In addition, titration of the recovered catalyst gave a slightly lower loading of accessible amine (0.47 mmol g^{-1}) compared with a fresh unspent sample of catalyst **2e** (0.61 mmol g^{-1}), indicating that some of the surface amine may have leached under the reaction conditions, which could account for the subtle changes in the textural properties. Future studies will further investigate the stability profile of **2e** in batch as well as in a packed bed reactor under continuous flow to fully understand why the activity and selectivity decrease on reuse.

The optimum protocol described above was also applied to the aqueous phase reduction of a selection of nitroarenes to explore the efficiency of **2e** across a range of substrates and to compare its performance against existing systems. Reactions were conducted at 50 °C for 3 h unless otherwise stated to obtain comparative data as a function of substrate, full detail of which are presented in Table 2. High conversions were obtained for nitroarenes substituted at the 4-position with electron donating groups including hydroxy-, methoxy-, *N,N*-dimethylamino, amino and methyl (Table 2, entries 2–6). While 4-nitroanisole, 4-nitrotoluene, *N,N*-dimethylnitroaniline and 4-nitroaniline reached 95%, 98%, >99% and 98% conversion, respectively, after only 3 h, the reduction of 4-nitrophenol required 19 h to achieve a comparable conversion. The reduction of nitroarenes containing electron withdrawing groups also gave good conversion to the corresponding aniline. For example, 4-chloronitrobenzene gave high conversion to afford 4-chloroaniline as the sole product with no evidence for competing hydrodehalogenation to either nitrobenzene or aniline under these conditions (Table 2, entry 7). The reduction of nitroarenes containing reducible functional groups such as cyano and methyl ester occurred with high conversion and complete chemoselectivity for the nitro group. For example, the reduction of 4-nitrobenzonitrile and methyl 4-nitrobenzoate resulted in high conversion to afford 4-aminobenzonitrile and methyl 4-aminobenzoate, respectively, as the sole products after 3 h (Table 2, entries 8–9). Not surprisingly, the reduction of 4-nitroacetophenone resulted in reduction of both the carbonyl and nitro group to afford 1-(4-aminophenyl)ethan-1-ol as the sole product at complete conversion with no evidence for 4-aminoacetophenone (Table 3, entries 10). Under the same conditions, reduction of the sterically more challenging 2-nitroacetophenone resulted in complete consumption of the substrate to afford a mixture of 1-(2-nitrophenyl)ethan-1-ol (16%) and 1-(2-aminophenyl)ethan-1-ol (84%) after 3 h (Table 3, entry 11), however, quantitative reduction to the amine could be achieved by extending the reaction time. When the reduction of 2- and 4-nitroacetophenone was conducted at 25 °C, under otherwise identical conditions, the acyl group in both substrates was rapidly and quantitatively reduced to afford 1-(2-nitrophenyl)ethan-1-ol and 1-(4-nitrophenyl)ethan-1-ol as the major product together with only a minor amount of the corresponding aniline after 60 min. Complete reduction to the corresponding arylamine was then achieved by adding a further five equivalents of dimethylamine borane and raising the reaction temperature to 50 °C for 1 h. Reassuringly, a reduction conducted with acetophenone as the substrate and DMAB as the hydrogen donor confirmed that conversion to 1-phenylethanol was complete after only 1 h at 30 °C in the absence of catalyst. Sterically demanding substates such as 2-methyl and 2-methoxy substituted nitroarenes also gave high conversions after 3 h, (Table 2, entries 12–13). However, reduction of the sterically congested 8-nitroquinoline was markedly more sluggish and only reached 31% conversion to 8-aminoquinoline after 20 h at 80 °C (Table 2, entry 14). Finally, the transfer hydrogenation of 6-nitrobenzothiazole also resulted in rapid reduction to afford 6-aminobenzothiazole with 100% selectivity at 97% conversion after 3 h (Table 2, entries 15).

© 2024 The Authors. ChemCatChem published by Wiley-VCH GmbH

18673899, 2024, 13, Downloaded from https://chemistry-europe.onlinelibrary.wiley.com/doi/10.1002/cctc.202400013 by Imperial College London, Wiley Online Library on [10/09/2025]. See the Terms and Conditions (https://onlinelibrary.wiley.com/terms-and-conditions) on Wiley Online Library for rules of use; OA articles are governed by the applicable Creative Commons License

Table 3. Aqueous phase reduction of nitroarenes to the corresponding aniline with dimethylamine borane using 0.5 mol% **2 e**.[a]

Entry	Substrate	Product	Conversion (%)[b]	Yield (%)[c]	Selectivity (%)[d]
1			100	78%	100
2[e]	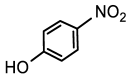	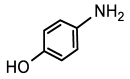	99	72%	>99
3	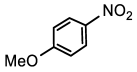	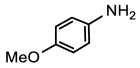	95	87%	96
4	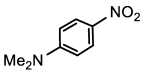	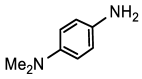	>99	89%	100
5	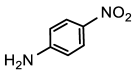	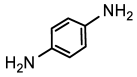	98	71%	100
6	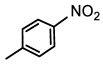	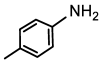	98	94%	100
7	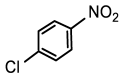	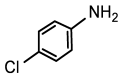	95	83%	100
8	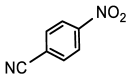	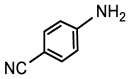	98	73%	84
9	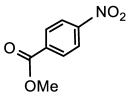	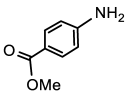	94	79%	100
10	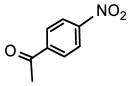	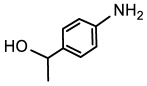	100	92%	100
11			100	71%	84[f]
12			98	89%	>99
13			100	87%	>99
14			31	24%	100
15	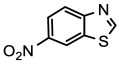	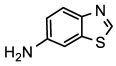	97	87%	100

[a] *Reaction conditions*: Conducted under nitrogen, 1.0 mmol substrate, 0.5 mol% **2 e**, 1 mL water, 4.0 mmol NMe_2HBH_3, 3 h, 50 °C. [b] % Conversion determined by ^{1}H NMR spectroscopy using 1,4-dioxane as internal standard. Average of at least three runs. [c] Yield determined from the selectivity and the mass of isolated material after aqueous workup. Selectivity for the arylamine [% arylamine / (% *N*-arylhydroxylamine + % azoxyarene + % azoarene + % hydrazoarene + % arylamine)]×100%. [e] Reaction time 19 h. [f] Selectivity based on the ratio of 1-(2-nitrophenyl)ethan-1-ol (16%) to 1-(2-aminophenyl)ethan-1-ol (84%).

Conclusions

RuNPs stabilised by mesoporous COK-12 modified with a primary amine and an imidazolium based ionic liquid (RuNP@NH_2-OMSIIL) is an efficient solvent dependent selective catalyst for the sodium borohydride-mediated reduction of nitrobenzene, giving hydrazobenzene as the major product in ethanol and aniline as the sole product in water, under otherwise identical conditions. In contrast, the same catalyst affords aniline as the sole product in both ethanol and water

© 2024 The Authors. ChemCatChem published by Wiley-VCH GmbH

18673899, 2024, 13, Downloaded from https://chemistry-europe.onlinelibrary.wiley.com/doi/10.1002/cctc.202400013 by Imperial College London, Wiley Online Library on [10/09/2025]. See the Terms and Conditions (https://onlinelibrary.wiley.com/terms-and-conditions) on Wiley Online Library for rules of use; OA articles are governed by the applicable Creative Commons License

when dimethylamine borane is used as the hydrogen donor. The initial TOF of 320 h^{-1} obtained for the selective partial reduction of nitrobenzene to hydrazobenzene is the highest to be reported with a nanoparticle-based catalyst and the first example that uses DMAB as the hydrogen donor. Under optimum conditions a range of substituted nitroarenes were reduced to the corresponding hydrazoarene with high selectivity in ethanol while the arylamine was obtained as the sole product in water. A survey of the catalyst efficacy as a function of the polymer composition revealed that removal of the amine resulted in a dramatic decrease in activity as did substitution of the primary amine for a tertiary amine; both modifications underpin the key role of the amine-modified support in enhancing catalyst performance. To this end, significant improvements in the efficacy of NP-based catalyst with amine-modified supports have recently been reported and attributed to several factors including; effective dispersion of the NPs, modification of the surface electronic structure of the NP, control of the size or a cooperative role in the elementary steps of the catalysis.[21m,n,q,39] While recycle studies resulted in a drop in conversion after the first run, analysis of the solvent indicated that this reduction was unlikely to be due to leaching or aggregation and catalyst poisoning studies confirmed that the NPs were most likely passivated/deactivated by the aniline product. Kinetic studies, in operando surface investigations and further catalyst modifications are currently underway to develop an understanding of the factors that affect catalyst performance and selectivity to inform the design of more efficient catalysts.

Experimental Section

Synthesis of 1-(3-(triethoxysilyl)propyl)pyrrolidine. Pyrrolidine (1.0 g, 0.014 mol) and 3-chloropropyltriethoxysilane (3.39 g, 0.014 mol) were mixed in a dry Schlenk flask under nitrogen. The system was evacuated and backfilled with nitrogen five times and heated for 90 °C for 60 h. After cooling to room temperature, the resulting solid was triturated with dry diethyl ether five times, the solvent was removed by syringe each time and then the remaining solid was dried under vacuum at room temperature for 48 h to obtain the desired product as a yellow oil in 91 % yield (3.5 g). ^{1}H NMR (300 MHz, $CDCl_3$, δ): 3.74 (q, J = 6,2 Hz, 6H, OCH_2), 2.53 (m, 2H, NCH_2), 2.45 (m, 4H, NCH_2), 1.71 (m, J = 3.3 Hz, 4H, NCH_2CH_2), 1.57 (m, 2H, CH_2), 1.15 (t, J = 6.2 Hz, 9H, OCH_2CH_3), 0.47 (m, 2H, SiCH_2). ^{13}C NMR (75 MHz, $CDCl_3$, δ): 59.9 (CH_2), 58.3 (OCH_2), 53.4 (NCH_2), 23.4 (NCH_2), 22.1 (NCH_2), 18.2 (OCH_2CH_2), 8.3 (SiCH_2).

Synthesis of 1,2-dimethyl-3-(3-(triethoxysilyl)propyl)-1H-imidazol-3-ium Chloride. 1,2-Dimethylimidazole (2.28 g, 0.024 mol) and 3-chloropropyltriethoxy silane (5.7 g, 0.024 mol) were mixed in a dry Schlenk flask under nitrogen flow. The system was evacuated and backfilled with nitrogen five times repeatedly and heated for 60 h at 90 °C. After cooling to room temperature, the resulting solid was triturated with dry diethyl ether five times, the solvent was removed by syringe each time and then the remaining solid was dried under vacuum at room temperature for 48 h to obtain the title compound as a white solid in 95 % yield (7.60 g). ^{1}H NMR (300 MHz, $CDCl_3$, δ): 7.89 (d, J = 2.2 Hz, 1H, CH_3-N-CH), 7.48 (d, J = 2.1 Hz, 1H, CH-CH-N), 4.19 (t, J = 7.4 Hz, 2H, N-CH_2), 4.02 (s, 3H, CH_3-N), 3.75 (q, J = 7.0 Hz, 6H, CH_2-O), 2.77 (s, 3H, N=C-CH_3), 1.94-1.78 (m, 2H, CH_2-CH_2-CH_2), 1.15 (t, J = 7.0 Hz, 9H, CH_2-CH_3), 0.58–0.53 (m, 2H, CH_2-Si). ^{13}C NMR (75 MHz, $CDCl_3$, δ): 123.4, 121.0, 58.7, 50.4, 36.0, 23.8, 18.3, 10.4, 7.1. This data is consistent with that published in the literature. IR: ν_{max} cm^{-1}: 669, 765, 803, 959, 1072, 1164, 1205, 1253, 1321, 1386, 1539, 1588, 1628, 2888, 2936, 2975, 3247, 3371, 3444.

Synthesis of COK-12 (1 a). Following a literature procedure,[26] the triblock copolymer Pluronic P123 (14.35 g) was dissolved in deionized water (385 mL) and the mixture stirred at room temperature overnight until all the P123 had completely dissolved. To this solution was added, citric acid monohydrate (13.21 g, 62.87 mmol) and trisodium citrate (9.10 g, 30.97 mmol) to buffer the pH and the resulting surfactant solution was stirred at room temperature for 24 h. A solution of sodium silicate (37.30 g of a solution containing 27 wt% SiO_2, 165 mmol) was diluted with H_2O (108 mL) and added dropwise to the surfactant solution avoiding the formation of aggregates. The pH was measured prior to and after sodium silicate addition to confirm the synthesis occurred in the pH range 4–6. The solution was stirred for 5 min at 175–180 rpm after which time the resulting mixture was kept at room temperature (20 °C) without agitation for 24 h. After this step, the as-synthesized material was filtered, washed with water (3×150 mL) and dried in an oven overnight. The dry white powdery solid (24.8 g) was then continuously extracted with ethanol (150 mL) for 15 days using a Soxhlet extractor to remove the organic templating agent.

General procedure for the synthesis of ionic liquid and amine modified COK-12 supports 1 b-d. Following the procedure described above for the synthesis of COK-12, the triblock co-polymer Pluronic P123 (14.35 g) was dissolved in deionized water (385 mL) and the mixture stirred at room temperature overnight until all the P123 had completely dissolved. To this solution was added citric acid monohydrate (13.21 g, 62.87 mmol) and trisodium citrate (9.11 g, 30.97 mmol) and the resulting surfactant solution was stirred for 24 h. Sodium silicate solution (35.4 g of a solution containing 27 wt% SiO_2, 165 mmol) was diluted with water (102 mL) and added dropwise to the surfactant solution together with 5 mol% of the corresponding imidazolium silica precursor 1,2-dimethyl-3-(3-(triethoxysilyl)propyl)-1H-imidazol-3-ium chloride or 5 mol% of one of the amine silica precursors triethoxysilylpropylamine or 1-(3-(triethoxysilyl)propyl)pyrrolidine, avoiding the formation of aggregates. The pH was measured prior to and after sodium silicate addition to confirm the synthesis was conducted in the pH range 4–6. The solution was stirred for 5 min at 175–180 rpm and then kept at room temperature (20 °C) without agitation for 24 h. After this time, the as-synthesized material was filtered, washed with water (4×150 mL) and dried under vacuum oven overnight. The resulting white powder was continuously extracted with ethanol (150 mL) for 15 days using a Soxhlet extractor to remove the organic templating agent afford the corresponding ionic liquid and amine modified COK-12 supports **1 b–d**.

General procedure for the synthesis of hybrid ionic liquid-amine modified COK-12 supports 1 e–f. The ionic liquid-amine hybrid COK-12 supports **1 e–f** were prepared as described above by conducting the hydrolysis with sodium silicate solution (27 wt% SiO_2) diluted with water together with a mixture of 5 mol% each of 1,2-dimethyl-3-(3-(triethoxysilyl)propyl)-1H-imidazol-3-ium chloride and either triethoxysilylpropylamine or 1-(3-(triethoxysilyl)propyl)pyrrolidine.

General procedure for the synthesis of COK-12 and modified COK-12 stabilized ruthenium nanoparticles 2 a–f. A solution of $RuCl_3 \cdot 3H_2O$ (0.064 g, 0.3 mmol) in water (2 mL) was added to a mixture of the mesoporous silica material **1 a–f** (0.50 g) in water (5 mL). After stirring for 19 h at room temperature, the water was removed under reduced pressure to afford a grey solid which was resuspended in ethanol (5 mL) and treated dropwise with a solution

© 2024 The Authors. ChemCatChem published by Wiley-VCH GmbH

18673899, 2024, 13, Downloaded from https://chemistry-europe.onlinelibrary.wiley.com/doi/10.1002/cctc.202400013 by Imperial College London, Wiley Online Library on [10/09/2025]. See the Terms and Conditions (https://onlinelibrary.wiley.com/terms-and-conditions) on Wiley Online Library for rules of use; OA articles are governed by the applicable Creative Commons License

of $NaBH_4$ (0.07 g, 21 mmol) in water (2 mL). The resulting black suspension was stirred at room temperature overnight, filtered through a frit and the final black solid washed with water, ethanol and diethyl ether. The powder was then dried in an oven at 50 °C for 2 h to afford **2a** (0.52 g, 92%); **2b** (0.54 g, 92%); **2c** (0.50 g, 89%); **1d** (0.5 g, 89%); **2e** (0.50 g, 89%); **1f** (0.5, 89%) as black solids.

General procedure for the reduction of nitroarenes to arylamines. An oven dried Schlenk flask was cooled to room temperature and charged with catalyst (5 μmol, 0.5 mol%), dimethylamine borane (0.236 g, 4.0 mmol) and water (1 mL). After stirring the suspension for 5 min, nitroarene (1.0 mmol) was added and the mixture stirred at the allocated temperature for the appropriate time. The reaction mixture was diluted with deionized water, the product extracted with ethyl acetate (2×10 mL), the organic fractions combined, and the solvent removed under reduced pressure. The residue was analysed by ^{1}H NMR spectroscopy using dioxane as the internal standard to quantify the composition and determine the selectivity.

General procedure for the reduction of nitroarenes to the hydrazoarene. An oven dried Schlenk flask was cooled to room temperature and charged with catalyst **2e** (5 μmol, 0.5 mol%), $NaBH_4$ (0.151 g, 4.0 mmol) and ethanol (1 mL). After stirring the suspension for 5 min, nitroarene (1.0 mmol) was added and the mixture stirred at 70 °C for the appropriate time. The reaction mixture was diluted with deionized water, the product extracted with ethyl acetate (2 x 10 mL), the organic fractions combined, and the solvent removed under reduced pressure. The residue was analyzed by ^{1}H NMR spectroscopy, using dioxane as the internal standard to quantify the composition and determine the selectivity.

General procedure for the catalyst reuse study. Nitrobenzene (0.103 mL, 1.0 mmol) was reduced to aniline at 50 °C following the general procedure described above. After 1.5 h a 0.1 mL aliquot was removed and analyzed by ^{1}H NMR spectroscopy to determine the composition. The reaction flask was then recharged with a further portion of nitrobenzene and an additional four equivalents of dimethylamine borane (0.236 g, 4.0 mmol) and the procedure repeated. Following the 4th run the catalyst was isolated, washed with water (2×10 mL) and ethanol (2×10 mL) and analyzed by TEM.

Procedure for the hot filtration study. A reduction of nitrobenzene (0.103 mL, 1.0 mmol) to aniline with dimethylamine borane (0.236 g, 4.0 mmol) was conducted at 50 °C following the general procedure described above. After 30 minutes the reaction mixture was filtered through a 0.45-micron syringe filter into a clean Schlenk flask under an inert atmosphere. The filtered reaction mixture was then stirred at 50 °C for a further 65 minutes and the progress of the reaction monitored as a function of time by removing an aliquot every 20 min and analysing the composition by NMR spectroscopy.

General Procedure for the poisoning study as a function of pre-stirring time. An oven-dried Schlenk flask cooled to room temperature under vacuum, back-filled with nitrogen and charged with **2e** (0.0015 g, 5 μmol, 0.5 mol%), dimethylamine borane (0.236 g, 4.0 mmol), water (1 mL) and aniline (0.091 mL, 1.0 mmol) and the resulting mixture stirred for the allocated time (0, 20, or 40 min) to explore the effect of the build-up of aniline and pre-stirring time on catalyst efficacy. The reaction was initiated by the addition of nitrobenzene (0.103 mL, 1.0 mmol) and the mixture was left to stir for 1.5 h at 50 °C. The reaction mixture was diluted by addition of deionized water (5 mL), the product extracted with ethyl acetate (3×5 mL), the organic fractions collected, and the solvent removed under reduced pressure. The resulting residue was analysed by ^{1}H NMR spectroscopy using 1,4-dioxane as internal standard (1.0 mmol) to quantify the composition of starting material and products and determine the selectivity.

Acknowledgements

We gratefully acknowledge the Deanship of Scientific Research (DSR) at King Abdulaziz University, Jeddah, Saudi Arabia for funding this project (grant no: KEP-37-130-41). We also thank (Dr Tracey Davey) for the SEM images (Faculty of Medical Sciences, Newcastle University) and Zabeada Aslam and the Leeds electron microscopy and spectroscopy centre (LEMAS) at the University of Leeds for TEM analysis. This research was funded through a studentship (Anthony Griffiths) awarded by the Engineering and Physical Sciences Centre for Doctoral Training in Molecules to Product (EP/SO22473/1). The authors greatly acknowledge their support of this work. This article is dedicated to the memory of Professor Stephen A. Westcott (Canada Research Chair holder in the Department of Chemistry & Biochemistry, Mount Allison University, Canada) who recently passed away; a fantastic and inspired scientist, a great ambassador for chemistry teaching and research in Canada and across the globe, a selfless, generous, and kind human being but most of all a genuine, true and sincere friend who is greatly missed. This project was also funded by the Deanship of Scientific Research (DSR) at King Abdulaziz University, Jeddah, under grant no. (G: 013-665-1442). The authors, therefore, acknowledge with thanks DSR for technical and financial support.

Conflict of Interests

The authors declare no conflicts of interest.

Data Availability Statement

The data that support the findings of this study are available in the supplementary material of this article.

Keywords: supported catalysis · ruthenium nanoparticles, amino decorated COK-12 immobilised ionic liquid stabilised nanoparticles · transfer hydrogenation · selectivity · partial reduction · nitroarenes

[1] a) N. Ono, The Nitro Group in Organic Synthesis, Wiley-VCH, New York, 2001; b) H.-U Blaser and E. Schmidt, Heterogeneous Catalysis and Fine Chemicals, Vol 4, Elsevier, Amsterdam, 1997; c) Z. Rappoport, The Chemistry of Anilines, Wiley, 3007; d) H.-U. Blaser, *Science* **2006**, *313*, 312–313; e) H. K. Kadam, S. G. Tilve, *RSC Adv.* **2015**, *5*, 83391–83407; f) R. S. Downing, P. J. Kunkeler, H. Bekkum, *Catal. Today* **1997**, *37*, 121–136.

[2] a) P. Ruiz-Castillo, S. L. Buchwald, *Chem. Rev.* **2016**, *116*, 12564–12649; b) R. Dorel, C. P. Grugel, A. M. Haydl, *Angew. Chem. Int. Ed.* **2019**, *58*, 17118–17129; c) M. M. Heravi, Z. Kheilkordi, V. Zadsirjan, M. Heydari, M. Malmir, *J. Organomet. Chem.* **2018**, *861*, 17–104; d) D. S. Surry, S. L. Buchwald, *Angew. Chem. Int. Ed.* **2008**, *47*, 6338–6361; e) Y. Aubin, C. Fischmeister, C. M. Thomas, J. L. Renaud, *Chem. Soc. Rev.* **2010**, *39*,

© 2024 The Authors. ChemCatChem published by Wiley-VCH GmbH

18673899, 2024, 13, Downloaded from https://chemistry-europe.onlinelibrary.wiley.com/doi/10.1002/cctc.202400013 by Imperial College London, Wiley Online Library on [10/09/2025]. See the Terms and Conditions (https://onlinelibrary.wiley.com/terms-and-conditions) on Wiley Online Library for rules of use; OA articles are governed by the applicable Creative Commons License

4130–4145; f) C. Fischer, B. Koenig, *Belstein J. Org. Chem.* **2011**, *7*, 59–74; g) I. P. Beletskaya, A. V. Cheprakov, *Organometallics* **2012**, *31*, 7753–7808.

[3] a) H.-U. Blaser, H. Steiner, M. Studer, *ChemCatChem* **2009**, *1*, 210–221; b) P. Lara, K. Philippot, *Catal. Sci. Technol.* **2014**, *4*, 2445–2465; c) I. Nakamula, Y. Yamanoi, T. Imaoka, K. Yamamoto, H. Nishihara, *Angew. Chem. Int. Ed.* **2011**, *50*, 5830–5833; d) K. Xu, Y. Zhang, X. Chen, L. Huang, R. Zhang, J. Huang, *Adv. Synth. Catal.* **2011**, *353*, 1260–1264; e) N. Sakai, K. Fujii, S. Nabeshima, R. Ikeda, T. Konakahara, *Chem. Commun.* **2010**, *46*, 3173–3175; f) R. V. Jagadeesh, G. Wienhöfer, F. A. Westerhaus, A.-E. Surkus, M.-M. Pohl, H. Junge, K. Junge, M. Beller, *Chem. Commun.* **2011**, *47*, 10972–10974; g) S. M. Kelly, B. H. Lipshutz, *Org. Lett.* **2014**, *16*, 98–101; h) Z. Zhao, H. Yang, Y. Li, X. Guo, *Green Chem.* **2014**, *16*, 1274–1281; i) P. S. Rathore, R. Patidar, T. Shripathi, S. Thakore, *Catal. Sci. Technol.* **2015**, *5*, 286–295; j) M. M. Moghaddam, B. Pieber, T. Glasnov, C. O. Kappe, *ChemSusChem* **2014**, *7*, 3122–3131.

[4] a) P. Wang, H. Liu, J. Niu, R. Li, J. Ma, *Catal. Sci. Technol.* **2014**, *4*, 1333–1339; b) Y. M. Yamada, Y. Yuyama, T. Sato, S. Fujikawa Y Uozumi, *Angew. Chem. Int. Ed.* **2014**, *53*, 127–131; c) X. Liu, H.-Q. Li, S. Ye, Y. M. Liu, H. Y. He, Y. Cao, *Angew. Chem. Int. Ed.* **2014**, *53*, 7624–7628; d) S. G. Oh, V. Mishra, J. K. Cho, B.-J. Kim, H. S. Kim, Y.-W. Suh, H. Lee, H. S. Park, Y. J. Kim, *Catal. Commun.* **2014**, *43*, 79–83.

[5] a) V. Macho, L. Vojcek, M. Schmidtova, M. Harustiak, *J. Mol. Catal.* **1994**, *88*, 177–184; b) U. Sharma, P. Kumar, N. Kumar, V. Kumar, B. Singh, *Adv. Synth. Catal.* **2010**, *352*, 1834–1840; c) Q. Shi, R. Lu, K. Jin, Z. Zhang, D. Zhao, *Green Chem.* **2006**, *8*, 868–870; d) D. Cantillo, M. M. Moghaddam, O. C. Kappe, *J. Org. Chem.* **2013**, *78*, 4530–4542; e) L. Huang, P. Luo, W. Pei, X. Liu, Y. Wang, J. Wang, W. Xing, J. Huang, *Adv. Synth. Catal.* **2012**, *354*, 2689–2694.

[6] G. Rothenberg, Catalysis, Concepts and Green Applications, Wiley-VCH, Weinheim, 2008.

[7] a) A. Corma, P. Serna, *Science* **2006**, *313*, 332–334; b) A. Corma, P. Serna, P. Concepción, J. J. Calvino, *J. Am. Chem. Soc.* **2008**, *130*, 8748–8753; c) S. Cai, H. Duan, H. Rong, D. Wang, L. Li, W. He, Y. Li, *ACS Catal.* **2013**, *3*, 608–612; d) K. Layek, M. L. Kantam, M. Shirai, D. Nishio-Hamane, T. Sasaki, H. Maheswaran, *Green Chem.* **2012**, *13*, 3164–3174.

[8] a) R. A. Sheldon, *Chem. Tech.* **1994**, *24*, 38–47; b) P. Baumeister, H.-U. Blaser, M. Studer, *Catal. Lett.* **1997**, *49*, 219–222; c) U. Siegrist, P. Baumeister, H.-U. Blaser, M. Struder, Chem. Ind. (Dekker) 75 (1998) 207–218.

[9] G. Rothenberg, Catalysis, Concepts and Green Applications, Wiley-VCH, Weinheim, 2008.

[10] a) X. Li, R. R. Thakore, B. S. Takale, F. Gallou, B. H. Lipshutz, *Org. Lett.* **2021**, *23*, 8114–8118; b) J. Feng, S. Handa, F. Gallou, B. H. Lipshutz, *Angew. Chem. Int. Ed.* **2016**, *55*, 8979–8983; c) H. Pang, F. Gallou, H. Sohn, J. Camacho-Bunquin, M. Delferro, B. H. Lipshutz, *Green Chem.* **2018**, *20*, 130–135.

[11] a) R. Nandhini, B. S. Krishnamoorthy, G. Venkatachalam, *J. Organomet. Chem.* **2019**, *903*, 120984; b) W.-G. Jia, H. Zhang, T. Zhang, D. Xie, S. Ling, E.-H. Sheng, *Organometallics* **2016**, *35*, 503–512; c) S. Pachisia, R. Kishan, S. Yadav, R. Gupta, *Inorg. Chem.* **2021**, *60*, 2009–2022; d) W. -G Jia, Z.-B Wang X. -T Zhi, *Appl. Organomet. Chem.* **2020**, *34*, e5289.

[12] a) Nanoparticles and Catalysis, Ed: D. Astruc Wiley VCH 2007; b) Nanooparticles in Catalysis: Advances in Synthesis and Applications. Ed: K. Philippot, A. Roucoux. Wiley VCH, 2021; c) Nanocatalysis in Ionic Liquids, Ed: M. H. G. Prechtl. Wiley VCH, 2017; d) M. R. Axet, K. Philippot, *Chem. Rev.* **2020**, *120*, 1085–1145.

[13] a) H. Goesmann, C. Feldmann, *Angew. Chem. Int. Ed.* **2010**, *49*, 1362–1395; b) A. Roucoux, J. Schulz, H. Patin, *Chem. Rev.* **2002**, *102*, 3757–3778.

[14] a) X.-F. Yang, A. Wang, B. Qiao, J. Li, J. Liu, T. Zhang, *Acc. Chem. Res.* **2013**, *46*,1740–1748; b) Nanoparticles: From Theory to Applications. Ed: G. Schmid, Wiley-VCH, 2006, 1–359.

[15] For insightful reviews on encapsulated metal nanoparticles for catalysis see: a) C. Gao, F. Lyu, Y. Yin, *Chem. Rev.* **2021**, *121*, 834–881; b) M. Li, Y. Yang, D. Yu, W. Li, X. Ning, R. Wan, H. Zhu, J. Mao, *Nano Res.* **2023**, *16*, 3451–3474; c) M. Wang, Q. Yang, *Chem. Sci.* **2022**, *13*, 13291–13302; **Zeolites**: d) Y. Wang, C. Wang, L. Wang, L. Wang, F.-S. Xiao, *Acc. Chem. Res.* **2021**, *54*, 2579–2590; e) Q. Sun, N. Wang, Q. Bing, R. Si, J. Liu, R. Bai, P. Zhang, M. Jia, J. Yu, *Chem.* **2017**, *3*, 477–493; f) N. Wang, Q. Sun, R. Bai, X. Li, G. Guo, J. Yu, *J. Am. Chem. Soc.* **2016**, *138*, 7484–7487; g) Q. Sun, N. Wang, T. Zhang, R. Bai, A. Mayoral, P. Zhang, Q. Zhang, O. Terasaki, J. Yu, *Angew. Chem. Int. Ed.* **2019**, *58*, 18570–18576; h) M. Zahmakiran, S. Özkar, *Langmuir* **2009**, *25*, 2667–2678; i) Q. M. Sun, N. Wang, T. J. Zhang, R. Bai, A. Mayoral, P. Zhang, Q. Zhang, O. Terasaki, J. Yu, *Angew. Chem. Int. Ed.* **2019**, *58*, 18570–18576; j) Q. Sun, N. Wang, R. Bai, Y. Hui, T. Zhang, D. A. Do, P. Zhang, L. Song, S. Miao, J. Yu, *Adv. Sci.* **2019**, *6*, 1802350; **Metal Oxides**: k) Z. Tang, I. Surin, A. Rasmussen, F. Krumeich, E. V. Kondratenko, V. A. Kondratenko, J. Pérez-Ramírez, *Angew. Chem. Int. Ed.* **2022**, *61*, e202200772; l) S. Kumar, S. Singh, N. Mathur, P. Roy, H. Joshi, *Inorg. Chem.* **2023**, *62*, 3993–4002; m) K. Ma, W. Liao, W. Shi, F. Xu, Y. Zhou, C. Tang, J. Lu, W. Shen, Z. Zhang, *J. Catal.* **2022**, *407*, 104–114; n) M. J. Ndolomingo, R. Meijboom, *Catal. Lett.* **2019**, *149*, 2807–2822; o) D. Motta, F. Sanchez, K. Alshammari, L. E. Chinchilla, G. A. Botton, D. Morgan, T. Tabanelli, A. Villa, C. Hammond, N. Dimitratos, *J. Environmental Chem. Eng.* **2019**, *7*, 103381; **Molecularly Modified Silica**: p) N. Levin, L. Goclik, H. Walschus, N. Antil, A. Bordet, W. Leitner, *J. Am. Chem. Soc.* **2023**, *145*, 22845–22854; q) S. J. L. Anandaraj, L. Kang, S. DeBeer, A. Bordet, W. Leitner, *Small* **2023**, *19*, 2206806; r) A. Bordet, W. Leitner, *Acc. Chem. Res.* **2021**, *54*, 2144–2157; s) D. Kalsi, S. J. L. Anandaraj, M. Durai, C. Weidenthaler, M. Emondts, S. P. Nolan, A. Bordet, W. Leitner, *ACS Catal.* **2022**, *12*, 14902–14910; t) L. Luza, C. P. Rambor, A. Gual, F. Bernardi, J. B. Domingo, T. Grehl, P. Brüner, J. Dupont, *ACS Catal.* **2016**, *6*, 6478–6486; u) E. N. Kusumawati, T. Sasaki, *Chem. Rec.* **2019**, *19*, 2058–2068; v) A. Bordet, G. Moos, C. Weosh, P. Licence, K. L. Luska, W. Leitner, *ACS Catal.* **2020**, *10*, 13904–13912; w) L. Goclik, H. Walschus, A. Bordet, W. Leitner, *Green Chem.* **2022**, *24*, 2937–2945; x) A. Bordet, E. El Sayed, M. Sanger, K. J. Boniface, D. Kalsi, K. L. luska, P. G. Jessop, W. Leitner, *Nat. Chem.* **2021**, *13*, 916–922; y) K. Mori, S. Masuda, H. Tanaka, K. Yoshizawa, M. Che, H. Yamashita, *Chem. Commun.* **2017**, *53*, 4677–4680; **MOFs** z) T. Lin, H. Wang, C. Cui, W. Liu, G. Li, *Chem. Res. Chinese Universities* **2022**, *38*, 1309–1323; aa) L. Mohammadi, M. Hosseinfard, M. R. Vaezi, *ACS Omega* **2023**, *8*, 8505–8518; bb) M. Mukoyoshi, H. Kitagawa, *Chem. Commun.* **2022**, *58*, 10757–10767; cc) C. S. L. Koh, H. Y. F. Sim, S. X. Leong, S. K. Boong, C. Chong, X. Yi Ling, *ACS Materials Lett.* **2021**, *3*, 557–573; dd) F. Zheng, K. Wang, T. Lin, Y. Wang, G. Li, Z. Tang, *Acta Chimica Sinica* **2023**, *81*, 669–680; ee) S. Zhang, L. Zhou, M. Chen, *RSC Adv.* **2018**, *8*, 12282–12291; ff) D. D. Tuan, K.-Y. A. Lin, *Chem. Eng. J.* **2018**, *351*, 48–55**; Porous carbon:**gg) X. Qu, R. Jiang, Q. Li, F. Zeng, X. Zheng, Z. Xu, C. Chen, J. Peng, *Green Chem.* **2019**, *21*, 850–860; hh) Y.-Y. Cai, X.-H. Li, Y.-N. Zhang, X. Wei, K.-X. Wang, J.-S. Chen, *Angew. Chem. Int. Ed.* **2013**, *52*, 11822–11825; ii) F.-Z. Song, Q.-L. Zhu, X. Yang, W.-W. Zhan, P. Pachfule, N. Tsumori, Q. Xu, *Adv. Energy Mater.* **2018**, *8*, 1701416; jj) B. Zhu, R. Zou, Q. Xu, *Adv. Energy Mater.* **2018**, *8*, 1801193; kk) W. Chen, D. Li, C. Peng, G. Qian, X. Duan, D. Chen, X. Zhou *J. Catal.* **2017**, *356*, 186–196; ll) Y.-T. Li, X.-L. Zhang, Z.-K. Peng, P. Liu, X.-C. Zheng, *ACS Sustainable Chem. Eng.* **2020**, *8*, 8458–8468; mm) R. Ding, Q. Chen, Q. Luo, L. Zhou, Y. Wang, Y. Zhang, G. Fan, *Green Chem.* **2020**, *22*, 835–842; nn) S. Akbayrak, Z. Özçifçi, A. J. Tabak, *Colloid Surf. Sci.* **2019**, *546*, 324–332; oo) L. Yin, T. Zhang, K. Dai, B. Zhang, X. Xiang, H. Shang, *ACS Sustainable Chem. Eng.* **2021**, *9*, 822–832; **Porous Polymers**:pp) Q. Sun, Z. Dai, X. Meng, L. Wang, F.-S. Xiao, *ACS Catal.* **2015**, *5*, 4556–4567; qq) X. Shao, X. Miao, X. Yu, Wei Wang, X. Ji, *RSC Adv.* **2020**, *10*, 9414–9419; rr) P. Bhanja, A. Modak, A. Bhaumik, *ChemCatChem* **2019**, *11*, 244–257; ss) R. Tao, X. Ma, X. Wei, Y. Jin, L. Qiu, W. Zhang, *J. Mater. Chem. A* **2020**, *8*, 17360–17391; tt) Y.-L. Wan, Z. Zhang, C. Ding, L. Wen, *J. CO2 Util.* **2021**, *52*, 101673; uu) X. Fang, C. Liu, L. Yang, T. Yu, D. Zhai, W. Zhao, W.-q. Deng, *J. CO2 Util.* **2021**, *54*, 101778; vv) Z. Zhang, H. Gai, Q. Li, B. Feng, M. Xiao, T. Huang, *Chem. Eng. J.* **2022**, *429*, 13224; ww) Y. Lei, Z. Chen, G. Lan, R. Wang, X.-Y. Zhou, *New J. Chem.* **2020**, *44*, 3681; xx) C. Cui, R. Sa, Z. Hong, H. Zhong, R. Wang, *ChemSusChem* **2020**, *13*, 180–187; yy) Q. Song, D. Xu, W. D. Wang, J. Fang, X. Sun, F. Li, B. Li, J. Kou, H. Zhu, Z. Dong, *J. Catal.* **2022**, *406*, 19–27; zz) A. Roy, N. Haque, R. Chatterjee, S. Biswas, A. Bhaumik, M. Sarkar, S. M. Islam, *New J. Chem.* **2023**, *47*, 6673–6684; aaa) M. Kathiresan, *Chem. Asian J.* **2023**, *18*, e202201299; bbb) X. Zhou, Z. Wang, B. Yu, S. Kuang, W. Sun, Y. Yang, *Green Chem.* **2022**, *24*, 4463–4469; ccc) G. Li, S. Dong, P. Fu, Q. Yue, Y. Zhou, J. Wang, *Green Chem.* **2022**, *24*, 3433–3460; ddd) Y. Sang, Z. Shu, Y. Wang, L. Wang, D. Zhang, Q. Xiao, F. Zhou, J. Huang, *Appl. Surf. Sci.* **2022**, *585*, 152663.

[16] a) N. Wei, X. Zou, H. Huang, X. Wang, W. Ding, X. Lu, *Eur. J. Org. Chem.* **2018**, 209–214; b) G. D. Kalita, M. R. Das, P. Das, *Dalton Trans.* **2021**, *50*, 13483–13496; c) R. B. N. Baig, R. S. Varma, *ACS Sustainable Chem. Eng.* **2013**, *1*, 805–809; d) R. Hudson, V. Chazelle, M. Bateman, R. Roy, C.-J. Li, A. Moores, *ACS Sustainable Chem. Eng.* **2015**, *3*, 814–820; e) K. H. Liew, M. Rocha, C. Pereira, A. L. Pires, A. M. Pereira, M. A. Yarmo, J. C. Juan, R. M. Yusop, A. F. Peixoto, C. Freire, *ChemCatChem* **2017**, *9*, 3930–3941; f) D. V. Jawale, E. Gravel, C. Boudet, N. Shah, V. Geertsen, H. Li, I. N. N. Namboothiri, E. Doris, *Chem. Commun.* **2015**, *51*, 1739–1742; g) C. Antonetti, M. Oubenali, A. M. R. Galletti, P. Serpb, G. Vannucci, *Appl.*

© 2024 The Authors. ChemCatChem published by Wiley-VCH GmbH

18673899, 2024, 13, Downloaded from https://chemistry-europe.onlinelibrary.wiley.com/doi/10.1002/cctc.202400013 by Imperial College London, Wiley Online Library on [10/09/2025]. See the Terms and Conditions (https://onlinelibrary.wiley.com/terms-and-conditions) on Wiley Online Library for rules of use; OA articles are governed by the applicable Creative Commons License

Catal. A. **2012**, *421–422*, 99–107; h) P. Tomkins, E. Gebauer-Henke, W. Leitner, T. E. Müller, *ACS Catal.* **2015**, *5*, 203–209; i) S. Yue, X. Wang, S. Li, Y. Sheng, X. Zou, X. Lua, C. Zhang, *N. J. Chem.* **2020**, *44*, 11861–11869; j) N. M. Patil, T. Sasaki, B. M. Bhanage, *RSC Adv.* **2016**, *6*, 52347–52352; k) F. Leng, I. C. Gerber, P. Lecante, S. Moldovan, M. Girleanu, M. R. Axet, P. Serp, *ACS Catal.* **2016**, *6*, 6018–6024.

[17] a) T. W. van Deelen, C. H. Mejía, K. P. de Jong, *Nat. Catal.* **2019**, *2*, 955–970; b) C. Gao, F. Lyu, Y. Yin, *Chem. Rev.* **2021**, *121*, 834–881; c) K. Liu, R. Qin, N. Zheng, *J. Am. Chem. Soc.* **2021**, *143*, 4483–4499; d) M. Zahid, J. Li, A. Ismail, F. Zaera, Y. Zhu, *Catal. Sci. Technol.* **2021**, *11*, 2433–2445; e) Z. Cao, J. Bu, Z. Zhong, C. Sun, Q. Zhang, J. Wang, S. Chen, X. Xie, *Appl. Catal.* **2019**, *578*, 105–115; f) Z. Luo, G. Zhao, H. Pan, W. Sun, *Adv. Energy Mater.* **2022**, *12*, 2201395.

[18] Y. Wang, R. Qin, Y. Wang, J. Ren, W. Zhou, L. Li, J. Ming, W. Zhang, G. Fu, N. Zheng, *Angew. Chem. Int. Ed.* **2020**, *59*, 12736–12740.

[19] For a highly informative review on the impact of ligands on heterogeneous nanocatalysis see: L. Lu, S. Zou, B. Fang, *ACS Catal.* **2021**, *11*, 6020–6058.

[20] a) S. Jayakumar, A. Modak, M. Guo, H. Li, X. Hu, Q. Yang, *Chem. Eur. J.* **2017**, *23* 7791–7797; b) Z. Wang, H. Jiang, *RSC Adv.* **2015**, *5*, 34622–34629; c) H. Jiang, X. Zheng, *Catal. Sci. Technol.* **2015**, *5*, 3728–3734; d) J. L. Castlebou, E. Bresó-Femenia, P. Blondeau, B. Chaudret, S. Castillón, C. Claver, G. Cyril, *ChemCatChem* **2014**, *6*, 3160–3168; e) M. Ibrahim, M. A. S. Garcia, L. L. R. Vono, M. Guerrero, P. Lecante, L. M. Rossi, K. Philippot, *Dalton Trans.* **2016**, *45*, 17782–17791; f) Y. Lei, Z. Chen, G. Lan, R. Wang, X.-Y. Zhou, *N. J. Chem.* **2020**, *44*, 3681–3689; g) G. D. Kalita, P. Sarmah, P. Kr Saikia, L. Saikia, P. Das, *N. J. Chem.* **2019**, *43*, 4253–4260; h) L. Wu, Z.-W. Li, F. Zhang, Y.-M. He, Q.-H. Fan, *Adv. Synth. Catal.* **2008**, *350*, 846–862; i) I. Cano, A. M. Chapman, A. Urakawa, P. W. M. N. van Leeuwen, *J. Am. Chem. Soc.* **2014**, *136*, 2520–2528; j) N. Almora-Barrios, I. Cano, P. W. M. N. van Leeuwen, N. Lopez, *ACS Catal.* **2017**, *7*, 3949–3954; k) I. Cano, M. A. Huertos, A. M. Chapman, G. Buntkowsky, T. Gutmann, P. B. Groszewicz, P. W. M. N. van Leeuwen, *J. Am. Chem. Soc.* **2015**, *137*, 7718–7727; l) M. Guo, H. Li, Y. Ren, X. Ren, Q Yang Ca Li, *ACS Catal.* **2018**, *8*, 6476–6485; m) X. Ren, M. Guo, H. Li, C. Li, L. Yu, J. Liu, Q. Yang, *Angew. Chem. Int. Ed.* **2019**, *58*, 14483–14488; n) X. Cai, J. Nie, G. Yang, F. Wang, C. Ma, C. Lu, Z. Chen, *Mater. Lett.* **2019**, *240*, 80–83; o) R. Tao, X. Shen, Y. Hu, K. Kang, Y. Zheng, S. Luo, S. Yang, W. Li, S. Lu, Y. Jin, L. Qiu, W. Zhang, *Small* **2020**, *16*, 1906005; p) P. Kumar, A. Das, B. Maji, *Org. Biomol. Chem.* **2021**, *19*, 4174–4192; q) Y. Yang, T. Wang, X. Jing, G. Zhu, *J. Mater. Chem. A* **2019**, *7*, 10004–10009; r) Y. Xu, T. Wang, Z. He, M. Zhou, W. Yu, B. Shi, K. Huang, *Macromolecules* **2017**, *50*, 9626–9635; s) Z.-C. Ding, C.-Y. Li, J.-J. Chen, J.-H. Zeng, H.-T. Tang, Y.-J. Ding, Z.-P. Zhan, *Adv. Synth. Catal.* **2017**, *359*, 2280–2287; t) A. Kann, H. Hartmann, A. Besmehn, P. J. C. Hausoul, R. Palkovits, *ChemSusChem* **2018**, *11*, 1857–1865; u) X. Chen, H. Zhu, X. Song, H. Du, T. Wang, Z. Zhao, Y. Ding, *React. Kinet. Mech. Catal.* **2017**, *120*, 637–649.

[21] a) S. G. Kwon, G. Krylova, A. Sumer, M. M. Schwartz, E. E. Bunel, C. L. Marshall, S. Chattopadhyay, B. Lee, J. Jellinek, E. V. Shevchenko, *Nano Lett.* **2012**, *12*, 5382–5388; b) W. Long, N. A. Brunelli, S. A. Didas, E. W. Ping, C. W. Jones, *ACS Catal.* **2013**, *3*, 1700–1708; c) F. P. da Silva, J. L. Fiorio, L. M. Rossi, *ACS Omega* **2017**, *2*, 6014–6022; d) Z. Guo, C. Xiao, R. V. Maligal-Ganesh, L. Zhou, T. W. Goh, X. Li, D. Tesfagaber, A. Thiel, W. Huang, *ACS Catal.* **2014**, *4*, 1340–1348; e) I. Schrader, J. Warneke, J. Backenköhler, S. Kunz, *J. Am. Chem. Soc.* **2015**, *137*, 905–912; f) H. Liu, Q. Mei, S. Li, Y. Yang, Y. Y. Wang, H. Liu, L. R. Zheng, P. An, J. Zhang, B. Han, *Chem. Commun.* **2018**, *54*, 908–11; g) M. R. Axet, S. Conejero, I. C. Gerber, *ACS Appl. Nano Mater.* **2018**, *1*, 5885–5894; h) M. Guo, C. Li, Q. Yang, *Catal. Sci. Technol.* **2017**, *7*, 2221–2227; i) B. Wu, H. Huang, J. Yang, N. Zheng, G. Fu, *Angew. Chem. Int. Ed.* **2012**, *51*, 3440–3443; j) S. Rana S B Jonnalagadda, *RSC Adv.* **2017**, *7*, 2869–2879; k) Y. Cao, S. Mao, M. Li, Y. Chen, Y. Wang, *ACS Catal.* **2017**, *7*, 8090–8112; l) H. Zhong, M. Iguchi, M. Chatterjee, T. Ishizaka, M. Kitta, Q. Xu, H. Kawanami, *ACS Catal.* **2018**, *8*, 5355–5362; m) S. Masuda, K. Mori, Y. Futamura, H. Yamashita, *ACS Catal.* **2018**, *8*, 2277–2285; n) K. Mori, S. Masuda, H. Tanaka, K. Yoshizawa, M. Che, H. Yamashita, *Chem. Commun.* **2017**, *53*, 4677–4680; o) Y. Luo, Q. Yang, W. Nie, Q. Yao, Z. Zhang, Z.-H. Lu, *ACS Appl. Mater. Interfaces* **2020**, *12*, 8082–8090; p) L. Xu, F. Yao, J. Luo, C. Wan, M. Ye, P. Cui, Y. An, *RSC Adv.* **2017**, *7*, 4746–4752; q) K. Koh, M. Jeon, C. W. Yoon, T. Asefa, *J. Mater. Chem. A* **2017**, *5*, 16150–16161; r) K. Mori, Y. Futamura, S. Masuda, H. Kobayashi, H. Yamashita, *Nat. Commun.* **2019**, *4094*; s) Q. Zhang, Z. Zhu, X. Zhang, P. Li, Y. Huang, X. Luo, Z. Liang, *Int. J. Hydrogen Energy* **2019**, *44*, 16707–16717; t) Z. Tian, D.-L. Chen, T. He, P. Yang, F.-F. Wang, Y. Zhong, W. Zhu, *Phys. Chem. Chem. Phys.* **2019**, *123*, 22114–22122.

[22] a) S. Doherty, J. G. Knight, T. Backhouse, E. Abood, H. Al-shaikh, A. R. Clemmet, J. R. Ellison, R. A. Bourne, T. W. Chamberlain, R. Stones, N. J. Warren, I. J. S. Fairlamb, K. R. J. Lovelock, *Adv. Synth. Catal.* **2018**, *360*, 3716–3731; b) S. Doherty, J. G. Knight, T. Backhouse, E. Abood, H. Al-shaikh, I. J. S. Fairlamb, R. A. Bourne, T. W. Chamberlain, R. Stones, *Green Chem.* **2017**, *19*, 1635–1641; c) S. Doherty, J. G. Knight, T. Backhouse, A. Bradford, F. Saunders, R. A. Bourne, T. W. Chamberlain, R. Stones, A. Clayton, K. R. J. Lovelock, *Catal. Sci. Technol.* **2018**, *8*, 1454–1467; d) S. Doherty, J. G. Knight, T. Backhouse, R. J. Summers, E. Abood, W. Simpson W Paget, R. A. Bourne, T. W. Chamberlain, R. Stones, K. R. J. Lovelock, J. M. Seymour, M. A. Isaacs, C. Hardacre H Daly, N. H. Rees, *ACS Catal.* **2019**, *9*, 4777–4791; e) S. Doherty, J. G. Knight, T. Backhouse, T. S. T. Tran, R. Paterson, F. Stahl, H. Y. Alharbi, T. W. Chamberlain, R. A. Bourne, R. Stones, A. Griffiths, J. P. White, Z. Aslam, C. Hardacre, H. Daly, J. Hart, R. H. Temperton, J. N. O'Shea, N. H. Rees, *Catal. Sci. Technol.* **2022**, *12*, 3549–3567; f) S. Doherty, J. G. Knight, H. Y. Alharbi, R. Paterson, C. Wills, C. Dixon, L. Šiller, T. W. Chamberlain, A. Griffiths, S. M. Collins, K. Wu, M. D. Simmons, R. A. Bourne, K. R. J. Lovelock, J. M. Seymour, *ChemCatChem* **2022**, *14*, e202101752; g) S. Doherty, J. G. Knight, R. Paterson, A. Alharbi, C. Wills, C. Dixon, L. Šiller, T. W. Chamberlain, A. Griffiths, S. M. Collins, K.-J. Wu, M. D. Simmons, R. A. Bourne, K. R. J. Lovelock, J. Seymour, *J. Mol. Catal.* **2022**, *528*, 112476; h) A. A. Alharbi, C. Wills, T. W. Chamberlain, R. A. Bourne, A. Griffiths, S. M. Collins, K.-J. Wu, M. D. Simmons, J. G. Knight, S. Doherty, *ChemCatChem* **2023**, *15*, e202300418; i) R. Paterson, C. Wills, T. W. Chamberlain, A. Griffiths, S. M. Collins, K.-J. Wu, M. D. Simmons, J. G. Knight, S. Doherty, *J. Catal.* **2023**, *417*, 74–86; j) S. Doherty, R. Paterson, L. E. Fahy, E. Arca, C. Dixon, C. Y. Wills, H. Yan, A. Griffths, S. M. Collins, K. Wu, R. A. Bourne, T. W. Chamberlain, J. G. Knight, *Chem. Commun.* **2023**, *59*, 13470–13473.

[23] For an insightful review, describing the use of covalently supported ionic liquids as supports in catalysis see: a) F. Giacalone, M. Gruttadauria, *ChemCatChem* **2016**, *8*, 664–684; b) V. Campisciano, F. Giacalone, M. Gruttadauria, *Chem. Rec.* **2017**, *17*, 918–938; c) For a review on Functionalized Ionic Liquids for the Synthesis of Metal Nanoparticles and their Application in Catalysis seeK. L. Luska, A. Moores, *ChemCatChem* **2012**, *4*, 1534–1546; d) K. L. Luska, P. Migowskia, W. Leitner, *Green Chem.* **2015**, *17*, 3195–3206.

[24] a) A. Singh, H. Hakk, S. J. Lupton, *J. Labelled Compd. Radiopharm.* **2018**, *61*, 386–390; b) S. A. Nour, N. S. Abdelmalek, M. J. Naguib, *Drug Delivery* **2015**, *22*, 286297; c) D. Gong, D. Kong, N. Xu, Y. Hua, B. Liu, Z. Xu, *Org. Lett.* **2022**, *24*, 7339–7343; d) M. K. Sahoo, G. Sivakumar, S. Jadhav, S. Shaikh, E. Balaraman, *Org. Biomol. Chem.* **2021**, *19*, 5289–5293.

[25] a) Y. Ma, Z. Lang, J. Du, L. Yan, Y. Wang, H. Tan, S. U. Khan, Y. Liu, Z. Kang, Y. Li, *J. Catal.* **2019**, *377*, 174–182; b) Q. Liu, Y. Xu, X. Qiu, C. Huang, M. Liu, *J. Catal.* **2019**, *370*, 55–60; c) N. Sakai, K. Fujii, S. Nabeshima, R. Ikeda, T. Konakahara, *Chem. Commun.* **2010**, *46*, 3173–3175; d) J. E. Hong, Y. Jung, Y. Park, Y. Park, *Highly ACS Omega* **2020**, *5*, 7576–7583; e) L. Chang, J. Li, N. Wu, X. Cheng, *Org. Biomol. Chem.* **2021**, *19*, 2468–2472.

[26] a) J. Jammaer, A. Aerts, J. D'Haen, J. W. Seo, J. A. Martens, *Stud. Surf. Sci. Catal.* **2010**, *175*, 681–684; b) J. Jammaer, A. Aerts, J. D'Haen, J. W. Seo, J. A. Martens, *J. Mater. Chem.* **2009**, *19*, 8290–8293.

[27] a) R. Joseph, S. Zhang, W. Ford, *Macromolecules* **1996**, *29*, 1305–1312; b) C. Calabrese, L. F. Liotta, F. Giacalone, M. Gruttadauria, C. Aprile, *ChemCatChem* **2019**, *11*, 560–567.

[28] a) A. Bordoloi, S. Sahoo, F. Lefebvre, S. B. Halligudi, *J. Catal.* **2008**, *259*, 232–239; b) B. Karimi, D. Elhamifar, J. H. Clark, A. J. Hunt, *Chem. Eur. J.* **2010**, *16*, 8047–8053; c) B. Karimi, M. Khorasani, F. B. Rostami, D. Elhamifar, H. Vali, *ChemPlusChem* **2015**, *80*, 990–999; d) C. Calabrese, V. Campisciano, F. Siragusa, L. F. Liotta, C. Aprile, M. Gruttadauria, F. Giacalone, *Adv. Synth. Catal.* **2019**, *361*, 3758–3767.

[29] a) B. Karimi, M. Gholinejad, M. Khorasani, *Chem. Commun.* **2012**, *48*, 8961–8961; b) Q. Li, T. Huang, Z. Zhang, M. Xiao, H. Gai, Y. Zhou, H. Song, *J. Mol. Catal.* **2021**, *509*, 111644; c) B. Feng, Z. Zhang, J. Wang, D. Yang, Q. Li, Y. Liu, H. Gai, T. Huang, H. Song, *Fuel* **2022**, *325*, 124853; d) H. Song, Y. Wang, Y. Liu, L. Chen, B. Feng, X. Jin, Y. Zhou, T. Huang, M. Xiao, F. Huang, H. Gai, *ACS Sustainable Chem. Eng.* **2021**, *9*, 2115–2128; e) K. Mori, S. Masuda, H. Tanaka, K. Yoshizawa, M. Chee, H. Yamashita, *Chem. Commun.* **2017**, *53*, 4677–4680; f) Q. Zhang, Z. Zhu, X. Zhang, P. Li, Y. Huang, X. Luo, Z. Liang, *Int. J. Hydrogen Energy* **2019**, *44*, 16707–16717; g) Z. Wang, H. Ge, X. Wang, C. Ye, S. Fan, *RSC Adv.* **2019**, *9*, 32425–32434.

[30] D. J. Morgan, *Surf. Interface Anal.* **2015**, *47*, 1072–1079.

© 2024 The Authors. ChemCatChem published by Wiley-VCH GmbH

18673899, 2024, 13, Downloaded from https://chemistry-europe.onlinelibrary.wiley.com/doi/10.1002/cctc.202400013 by Imperial College London, Wiley Online Library on [10/09/2025]. See the Terms and Conditions (https://onlinelibrary.wiley.com/terms-and-conditions) on Wiley Online Library for rules of use; OA articles are governed by the applicable Creative Commons License

[31] E. Moaseri, M. Baniadam, M. Maghrebi, M. Karimi, *Chem. Phys. Lett.* **2013**, *555*, 164–167.
[32] a) M. Zhao, L. Xu, M. Vara, A. O. Elnabawy, K. D. Gilroy, Z. D. Hood, S. Zhou, L. Figueroa-Cosme, M. Chi, M. Mavrikakis, Y. Xia, *ACS Catal.* **2018**, *8*, 6948–6960; b) H. Ye, Q. Wang, M. Catalano, N. Lu, J. Vermeylen, M. J. Kim, Y. Liu, Y. Sun, X. Xia, *Nano Lett.* **2016**, *16*, 2812–2817; c) Y. Zhao, Y. Luo, X. Yang, Y. Yang, Q. Song, *J. Hazard. Mater.* **2017**, *332*, 124–131; d) C. Wang, R. Ciganda, L. Salmon, D. Gregurec, J. Irigoyen, S. Moya, J. Ruiz, D. Astruc, *Angew. Chem. Int. Ed.* **2016**, *55*, 3091–3095; e) N. C. Antonels, R. Meijboom, *Langmuir* **2013**, *29*, 13433–13442; f) E. Murugan, I. Pakrudheen, *Adv. Mater.* **2015**, *7*, 891–901; g) J. Mondal, S. K. Kundu, W. K. H. Ng, R. Singuru, P. Borah, H. Hirao, Y. Zhao, A. Bhaumik, *Chem. Eur. J.* **2015**, *21*, 19016–19027; h) J. H. Tyler, S. H. Nazari, R. H. Patterson, V. Udumula, S. J. Smith, D. J. Michaelis, *Tet. Lett.* **2017**, *58*, 82–86; i) J. Zhang, L. Pei, J. Wang, P. Zhu, X. Gu, Z. Zheng, *Catal. Sci. Technol.* **2020**, *10*, 1518–1528.
[33] Z. Yan, X. Xie, Q. Song, F. Ma, X. Sui, Z. Huo, M. Ma, *Green Chem.* **2020**, *22*, 1301–1307.
[34] a) E. A. Gelder, S. D. Jackson, C. M. Lok, *Chem. Commun.* **2005**, 522–524; b) A. Corma, P. Concepción, P. Serna, *Angew. Chem. Int. Ed.* **2007**, *46*, 7266–7269; c) F. Haber, *Z. Elektrochem.* **1898**, *22*, 506.
[35] a) D. Bhattacherjee, Shaifali, A. Kumar, G. V. Zyryanov, P. Das, *Mol. Catal.* **2021**, *514*, 111836; b) V. Udumula, J. H. Tyler, D. A. Davis, H. Wang, M. R. Linford, P. S. Minson, D. J. Michaelis, *ACS Catal.* **2015**, *6*, 3457–3462; c) D. Nandi, S. Siwal, M. Choudhary, K. Mallick, *Appl. Catal. A General* **2016**, *523*, 31–38; d) Y.-M. Lu, H.-Z. Zhu, W.-G. Li, B. Hu, S.-H. Yu, *J. Mater. Chem. A* **2013**, *1*, 3783–3788; e) B. Lakshminarayana, G. Satyanarayana, C. Subrahmanyam, *ACS Omega* **2018**, *3*, 13065–13072; f) A. K. Shil, P. Das, *Green Chem.* **2013**, *15*, 3421–3428.
[36] a) E. Vasilikogiannaki, C. Gryparis, V. Kotzabasaki, I. N. Lykakis, M. Stratakis, *Adv. Synth. Catal.* **2013**, *355*, 907–911; b) S.-C. A Lin, Y.-H. Liu, S.-M. Peng, S.-T. Liu, *J. Mol. Catal.* **2019**, *466*, 46–51; c) E. H. Boymans, P. T. Witte, D. Vogt, *Catal. Sci. Technol.* **2015**, *5*, 176–183.
[37] a) R. Breslow in The Principles of and Reasons for Using Water as a Solvent for Green Chemistry Wiley-VCH, 2009 pp 1–29; b) M. Cortes-Clerget, J. Yu, J. R. A. Kincaid, P. Walde, F. Gallou B H Lipshutz, *Chem. Sci.* **2021**, *12*, 4237–4266.
[38] a) G. Chen, C. Xu, X. Huang, J. Ye, L. Gu, G. Li, Z. Tang, B. Wu, H. Yang, Z. Zhao, Z. Zhou, G. Fu, N. Zheng, *Nat. Commun.* **2016**, *15*, 564–569; b) Y. Takenaka, T. Kiyosu, J.-C. Choi, T. Sakakura, H. Yasuda, *Green Chem.* **2009**, *11*, 1385–1390.
[39] a) S. Masuda, K. Mori, Y. Kuwahara, H. Yamashita, *J. Mater. Chem. A* **2019**, *7*, 16356–16363; b) X. Lv, G. Lu, Z.-Q. Wang, Z.-N. Xu, G.-C. Guo, *ACS Catal.* **2017**, *7*, 4519–4526; c) S.-J. Li, Y.-T. Zhou, X. Kang, D.-X. Liu, L. Gu, Q.-H. Zhang, J.-M. Yan, Q. Jiang, *Adv. Mater.* **2019**, *31*, 1806781.

Manuscript received: January 3, 2024
Revised manuscript received: February 28, 2024
Accepted manuscript online: March 7, 2024
Version of record online: March 22, 2024

© 2024 The Authors. ChemCatChem published by Wiley-VCH GmbH

18673899, 2024, 13, Downloaded from https://chemistry-europe.onlinelibrary.wiley.com/doi/10.1002/cctc.202400013 by Imperial College London, Wiley Online Library on [10/09/2025]. See the Terms and Conditions (https://onlinelibrary.wiley.com/terms-and-conditions) on Wiley Online Library for rules of use; OA articles are governed by the applicable Creative Commons License